Correlation of Gravity Anomalies with Precambrian Crystalline Basement, Bellefontaine Outlier, Ohio

A Senior Thesis

Submitted as Partial Fulfillment of the Requirements

for the degree Bachelor of Science in

Geological Sciences at

The Ohio State University

by

Christian D. Steck

• • • • •

The Ohio State University

Winter, 1997

Hallan C. Noltimier

Dr. Hallan C. Noltimier

Acknowledgments

I would like to extend my sincere thanks to everyone who has supported me during this project. Special thanks go to my thesis advisor, Dr. Hallan Noltimier, for his continuous encouragement, sound advice, and helpful suggestions. He made this an extremely pleasurable endeavor. I would also like to thank Larry Wickstrom of the Ohio Division of Geological Survey for providing his geological expertise and the materials produced by the Cincinnati Arch Consortium. Jim MacDonald, also of the Survey, and Jeoong-Woo Kim of the Ohio State University were also very beneficial resources for their geologic and computer-related support. Many thanks go to my friends and family for their encouragement and assistance. All have been invaluable to the completion of this thesis.

TABLE OF CONTENTS

LIST OF FIGURES

Figure | Page

LIST OF TABLES

INTRODUCTION

Reaching a height of 1549 ft at Campbell Hill, the Bellefontaine Outlier in Logan County is the highest point in Ohio. This highland is anomalous because it is surrounded by extensively glaciated terrain which covers most of northern and western Ohio. The Outlier consists of a block of Devonian shales and carbonates capped with Pleistocene till and surrounded by Silurian limestones, dolomites, and shales. Because of limited deep drilling in the area, the origin of the Outlier has been difficult to determine. It's flat-lying Paleozoic strata lies directly over the north-south trending Grenville Tectonic Front—thought to be the result of a Proterozoic plate collision about 1.0 Ga. The basement rocks east of the Grenville Front are Grenville Province metamorphics. To the west are Precambrian lithic sandstones and volcanics of the East Continent Rift Basin. Surrounding this basin to the north, south, and west lie Granite-Rhyolite Province igneous rocks. Seismic, potential field (gravity and magnetic), and well data have been used in the interpretation of the Outlier and surrounding region.

This study was a continuation of the field work and interpretations in Weaver (1992). My objective was to better determine the structural nature of the Precambrian crystalline basement surface underlying the Bellefontaine Outlier. This work was based on Complete Bouguer Residual Anomalies. In conjunction with recent regional studies of the Precambrian basement structure and lithology by the Cincinnati Arch Consortium, the anomalies were used to further define the locations and magnitudes of previously (and newly) identified basement faults. An introduction to the geology of the region and the Outlier is followed by an explanation of the gravity profiles and their significance. It is hoped that such information will be of future use in the further development of the tectonic origin and history of the Bellefontaine Outlier and Precambrian basement.

REGIONAL GEOLOGY

General Tectonic History

The formation of Laurentia, the North American protocontinent, began with the accretion of microcontinents in the Early Proterozoic. In Ohio, the oldest known events occurred during the mid Proterozoic (Keweenawan) between 1.4-1.5 Ga. At this time, the seven mile thick Granite-Rhyolite Province was emplaced, presumably the result of a mantle superswell. Crustal upwelling resulted in doming which caused rifting, producing the East Continent Rift Basin (ECRB) (Hansen, 1996). This, in turn, was filled (up to 20,000 ft thick in places) by basalt flows, rhyolitic volcanics, and erosion of the surrounding rocks. The ECRB is similar in configuration and age to Keweenawan rifts in Michigan, with which it may be continuous in subcrop. The basin is filled by the Middle Run Formation (Drahovzal et al., 1992). By about 1.0 Ga. the doming, rifting, volcanic activity, and basin filling had stopped. Alternative theories have related the basin in western Ohio to a foreland basin of the Grenville Mountains, or sedimentary rocks deposited with the igneous rocks in the Granite-Rhyolite Province, or faulting after the formation of the Grenville Mountains (Hansen, 1996).

Between 990-880 Ma., a continental collision on the eastern edge of North America (then in eastern Ohio) produced a 3,000 mile long orogenic belt, the Grenville Mountains. Today in eastern Ohio, west dipping seismic reflectors of the Coshocton Zone, have been interpreted to represent the suture zone between these colliding continents. The Grenville Front Tectonic Zone (GFTZ) represents the western extent of the deformation that produced the Grenville Mountains. It separates the 1.4-1.5 Ga. Granite-Rhyolite Province in the west from 990-880 Ma. metamorphics of the Grenville Province in the east (Hansen, 1996). The 30 mile wide GFTZ has a north-south strike, dips to the east. It has been interpreted as a series of imbricate thrusts and wrench faults. It is characterized by gravity and magnetic anomalies and metamorphism and thrusting across part of the rift zone in western Ohio (Hansen, 1996; Wickstrom, 1992).

During the Late Precambrian, there was an extended period (300 my) of erosion. The Grenville Mountains were worn away, probably removing the uppermost sedimentary rocks of the rift basin. There is also evidence of extensive strike-slip (wrench) faulting at this time. By the end of the Precambrian, about 570 Ma., a marine transgression initiated the deposition of the Paleozoic section (Hansen, 1996).

Three later tectonic events occurred during the Phanerozoic in Ohio. The Middle-Late Ordovician Taconic Orogeny, (475-440 Ma.) involved the closure of the Iapetus Ocean between Laurentia and Baltica. The collision involved Laurentia and an island arc, not Baltica itself, and was characterized by high-angle faults. The Late Devonian Acadian and Late Carboniferous Alleghenian Orogenies followed. These episodes involved the collision of Laurentia with the continents of Baltica and Africa respectively (Stanley, 1993).

Precambrian Section

Of primary importance to this study is the Precambrian basement. These rocks have the most significant influence on the gravity as well as the structure of the Bellefontaine Outlier. Figure 1 shows the location of the Study Area in Logan, Champaign, and Union Counties in Ohio. The map in Figure 2 identifies the Outlier within the fundamental geologic features in this region. Structure contours on the Precambrian crystalline basement, west of the Grenville Front, and on the Grenville Province, east of the Grenville Front are in Figure 3. The Study Area straddles a complex system of faults including the Grenville Front and series of high-angles faults within the East Continent Rift Basin.

Granite-Rhyolite Province

The top of the Proterozoic Granite-Rhyolite Province, or Central Province, is defined in the COCORP Seismic Line OH-1 as the top of the deepest, strong, planar, continuous reflectors above chaotic reflectors. At the Indiana border in west-central Ohio, the Granite-Rhyolite Province is about -2500 ft below mean sea level and plunges to -25,000 ft at the Grenville Front (Figure 4). In the survey area it lies between -7500 and -15,000 ft. It is buried beneath 5000-15,000 ft of the Middle Run Formation and associated volcanics of the East Continent Rift Basin (Wickstrom et al., 1992).

Figure 1. State of Ohio showing county boundaries, the Bellefontaine Outlier (shaded), and the Survey Area (box), modified from Wickstrom et al. (1992).

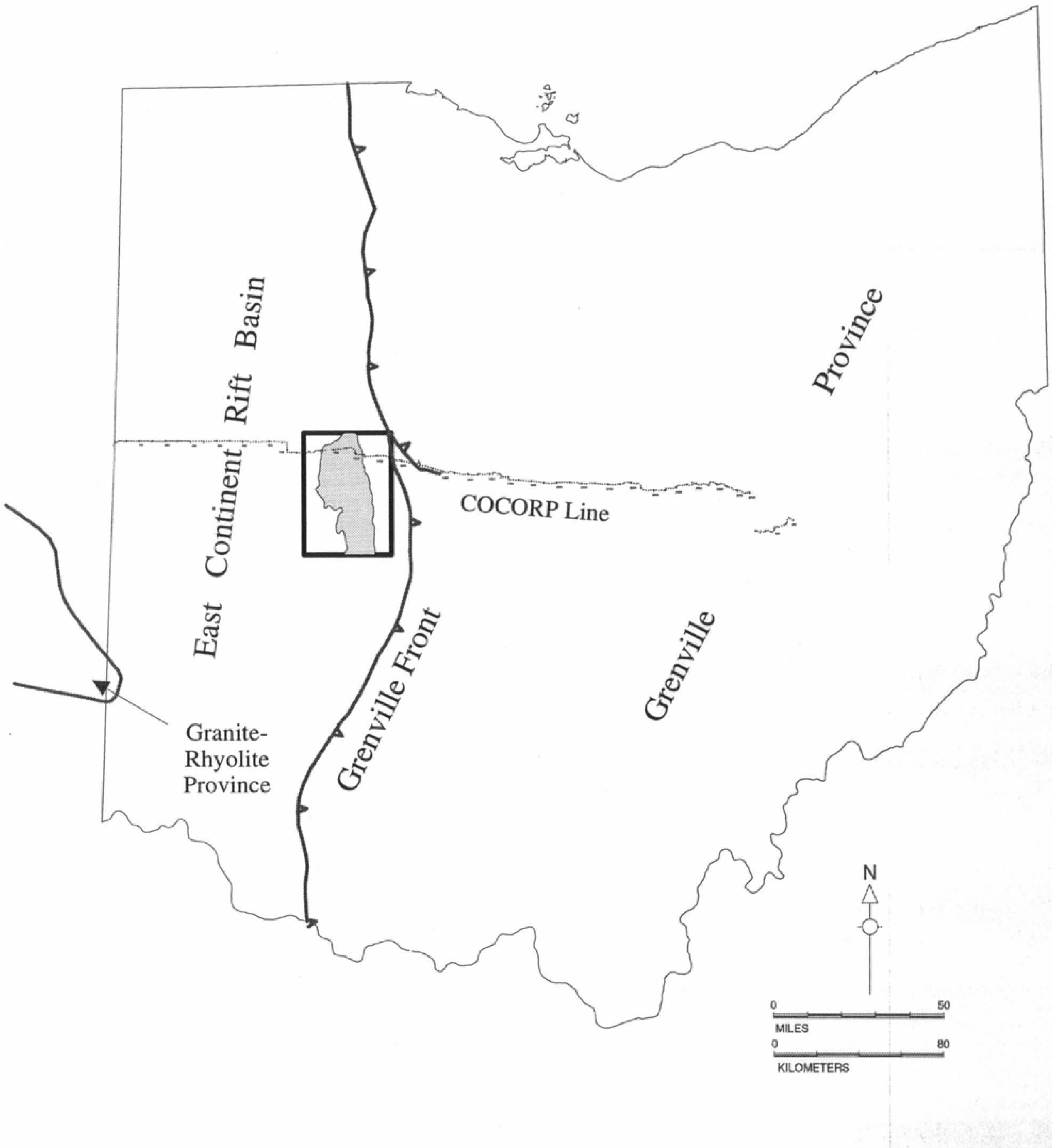

Figure 2. State of Ohio showing the Survey Area (box), the Bellefontaine Outlier (shaded), the Grenville Front, the Grenville Province, the Granite-Rhyolite Province, and the COCORP Seismic Line OH-1, modified from Wickstrom et al. (1992).

Geologic Time (million years before presen)	System	Series	Significant Stratigraphic Unit		Principal lithology	Thickness (feet)	
0	Quaternary	Pleistocene/ Holocene	Quaternary undifferentiated		glacial drift and alluvium	0-250+	Mappable units within the Bellefontaine Outlier
360	Devonian	Upper	Ohio Shale		carbonaceous shale, carbonaceous concretions at base	200+	
		Middle	Columbus-Lucas undifferentiated		dolomite, some sandy dolomite and chert	85-100	
408	Silurian	Upper	Salina undifferentiated		dolomites, some argillaceous or shaly	130-137	
			Tymochtee Dolomite		argillaceous or shaly dolomite	100	
			Greenfield Dolomite		dolomite	23-62	
		Lower	Lockport Dolomite		dolomite, some chert	63-113	
			Sub-Lockport undifferentiated		dolomites, some argillaceous or shaly, dolomitic shale, and limestone	60-175	
438	Ordovician	Cincinnatian	Ordovician undifferentiated		dolomitic shale and interbedded limestone and shale	300-400	
		Mohaw -kian	Trenton Limestone		limestone, dolomite		
			Black River Group				
			Wells Creek Formation				
505	Cambrian	St. Croixan	Knox Dolomite			500-750	
			Kerbel Formation				
			Eau Claire Formation			178	
			Rome Formation		dolomite	212	
			Mt. Simon Sandstone		sandstone	120	
570	Precambrian		Middle Run Formation (sandstone)	Grenville Province (metaigneous, igneous, and metasedimentary rocks)		Middle Run Fm: 5000-15,000	
			Granite-Rhyolite Province				

Figure 3. Generalized stratigraphic column in Bellefontaine Outlier Survey Area, modified from Hull, 1990; Swinford and Slucher, 1995.

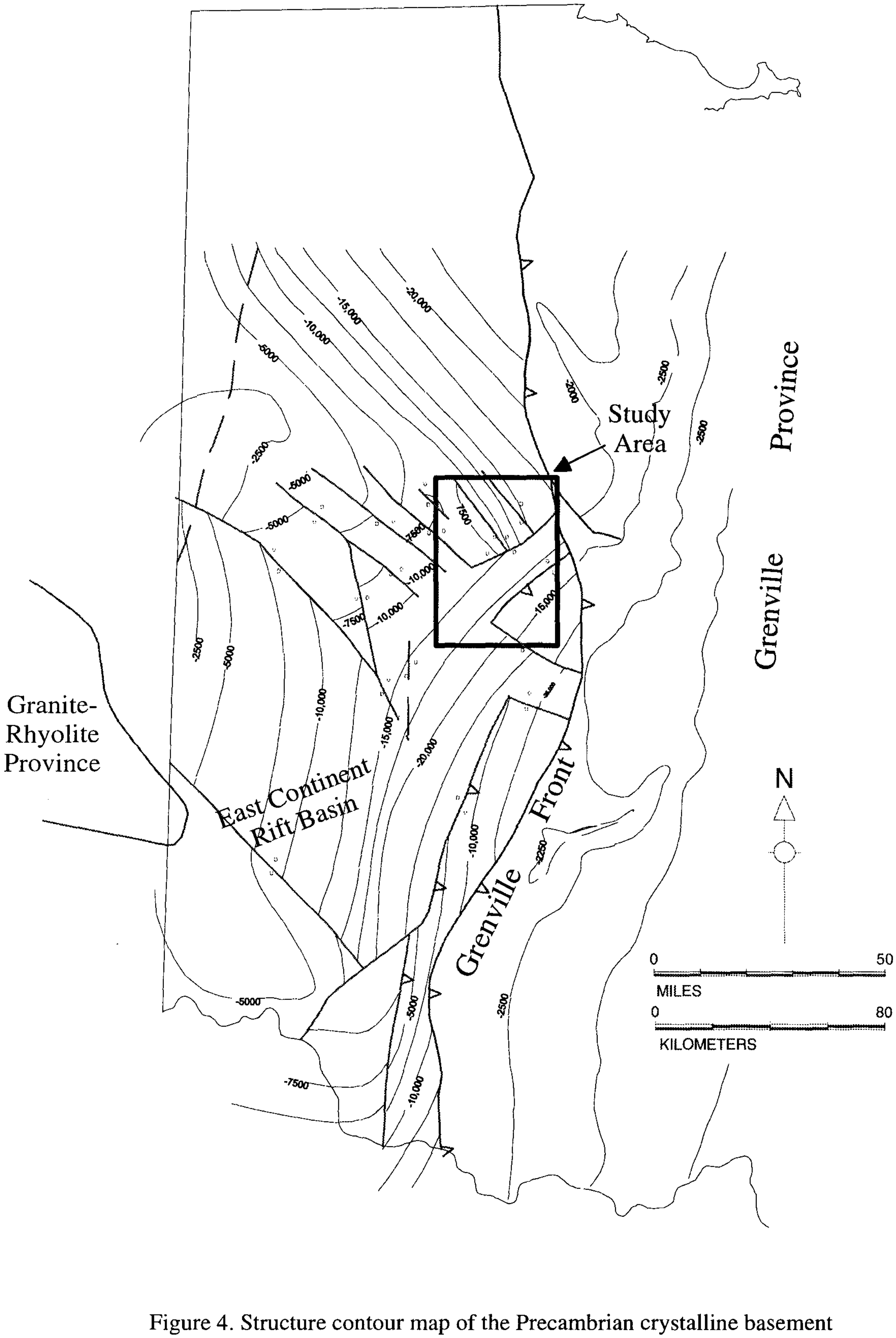

Figure 4. Structure contour map of the Precambrian crystalline basement surface in western Ohio. Contour interval is 2,500 ft. All depths below mean sea level. Modified from Wickstrom et al. (1992).

East Continent Rift Basin

The East Continent Rift Basin (ECRB) is filled by the Middle Run Formation. It extends from the Grenville Front in western Ohio and central Kentucky through south-central and northwestern Indiana. In the COCORP profile, seismic reflectors increase in strength and continuity from top to bottom in this section. The weaker reflectors are interpreted to be Middle Run alluvial sediments, the stronger reflectors interbedded basalt flows and siliciclastics. The ECRB is thickest (25,000 ft) at the Grenville Front in northwestern Ohio. The section thins to the west and has apparently been uplifted due to tectonic compression. It also seems to be divided into northern and southern subbasins by the Fort Wayne Rift. The seismic profile shows the section to be highly faulted, with up to 7000 ft of vertical throw on the largest fault. Alternative interpretations show imbricate thrusts parallel to and west of the Grenville Front. Much of the section is at an angle to the overlying Paleozoic section. This indicates some form of Grenville structure prior to the Late Proterozoic. The top of the section is flat and contains less faulting (Wickstrom et al., 1992).

The ECRB is adjacent to the Grenville Province in the east. Because of the complex nature of the Grenville Front Tectonic Zone, the true nature and location of the eastern boundary of the ECRB is as yet undetermined. It is thought to lie somewhere under the Grenville Front. Drahovzal et al. (1992) interpreted the ECRB and the Grenville Province contact to be a complex wrench-fault system, possibly obliterating any thrust relationship. Magnetic modeling and seismic interpretation indicate that the basin deepens to 27,000 ft below sea level under the Cincinnati Arch and the sediment and volcanic fill are up to 22,500 ft thick. In the north the ECRB may connect with Michigan MCR basins. The seismic properties and stratigraphy of the ECRB are similar to the mid-Proterozoic (Keweenawan) MRS. The southern boundary is poorly defined. It may extend and narrow into central Tennessee. In the west, the boundary is thought to be limited by tilted GRP blocks, but it may extend beneath the Illinois Basin. Faults in the ECRB are thought to be due to the Keweenawan rifting or the subsequent Grenville compression, some have probably been active during multiple events (Drahovzal et al., 1992).

Grenville Front Tectonic Zone

The location of the Grenville Front Tectonic Zone (GFTZ) has been estimated with seismic, gravity, magnetic, and well data. Nevertheless, its relationship to surrounding rocks is somewhat difficult to define. The region has been subject to intense crustal stresses resulting from several episodes of plate collision. Compression during the Grenville Orogeny produced thrusting which was later overprinted by Late Proterozoic and possibly early Cambrian wrench faulting. In Kentucky, it is described as an overthrust, later modified by wrench-tectonic movement. It is bordered by the Grenville Province to the east. To the west, the GFTZ is adjacent to the East Continent Rift Basin rather than to the Granite-Rhyolite Province (Wickstrom et al., 1992).

Grenville Province

The Proterozoic Grenville Province was identified in the COCORP profile from the strong, steep, discontinuous reflectors. The upper surface is the deepest, strong, flat, continuous reflector. Defractions to the east of the GF were interpreted as flower structures representing wrench faults (Wickstrom et al., 1992). In west-central Ohio, seismic reflectors in the Grenville Province within the GFTZ dip 25°-30° to the east. They are interpreted to be ductile deformation zones in the Grenville Front. In eastern Ohio, however, the reflectors dip about 40° to the west. This 100 mile wide structural feature, the Coshocton Zone, appears in COCORP line OH-2 and has been interpreted as a suture zone. It is also associated with large scale gravity and magnetic anomalies extending from western New York, through West Virginia, and into north-central Alabama (Culotta et al., 1990; Pratt et al., 1989).

Top of Precambrian unconformity

The top of the Precambrian section lies over the Grenville Province, the East Continent Rift Basin, and the Granite-Rhyolite Province where the GRP is not covered by the ECRB. This surface as it appears in Drahovzal et al. (1992) was mapped from abundant magnetic data, but very sparse well and seismic data. It is relatively gently and smoothly sloping in Ohio. In the western part of the state it is nearly flat, but drops steeply toward the Appalachian Basin to the east. In Kentucky it is broken by east-northeast normal faults resulting from extension of the Cambrian Rome Trough. Beneath the ECRB the degree of faulting is less intense. In Logan County, Ohio, the faults are subparallel to the Grenville Front. Under the Bellefontaine Outlier thickening of the Cambrian section indicates that there was reactivation or initial formation of at least some of these faults during the Cambrian. Cambrian reactivation did occur along the Grenville Front adjacent to the Rome Trough, throws there range from a few hundred up to 4000 ft (Wickstrom et al., 1992).

Top of Precambrian crystalline basement

The Precambrian crystalline basement can be divided into three parts relative to the East Continent Rift Basin: west, east, and subjacent. East of the ECRB and Grenville Front is the Grenville Province. In Ohio it dips southeast from -2500 down to -5000 ft in the north, to -12,000 ft in the south. To the west of the ECRB is the Granite-Rhyolite Province which ranges from -7500 to more than -25,000 ft near the Grenville Front and from -2500 to -12,500 ft near the Ohio-Indiana border. Subjacent to the ECRB are northeast and northwest oriented normal faults having throws from several hundred to 7000 ft (Wickstrom et al., 1992).

<u>Paleozoic Section</u>

At the base of the Paleozoic section are the Middle-Late Cambrian Mount Simon, Rome, and Conasauga Formations. They are generally flat but thicken to the east and the west. The thickness changes may suggest faulting in the Early and Middle Cambrian. Related faulting in Kentucky, although less intense, was associated with active subsidence and tectonic inversion. Part of these formations in the reprocessed COCORP Seismic Line OH-1 are interpreted as highly faulted and having an irregular basal contact with the Precambrian Middle Run Formation (Wickstrom et al., 1992).

Structural highs and reactivation of Precambrian faults and structures have influenced the deposition of Paleozoic sedimentary rocks, including the strata over the Bellefontaine Outlier (Wickstrom et al., 1992). Periodic fault reactivation has occurred up to the present along the Bowling Green Fault and the Fort Wayne (Anna-Champaign) Rift (Hansen, 1996).

In the Ohio, the Paleozoic section is represented by Cambrian through Permian age rocks, predominantly composed of dolomites and shales. There are no Mesozoic or Tertiary age sediments present. Overlying the Paleozoic bedrock are the most recent sediments, Pleistocene glacial deposits, which include the Wisconsinan, and presumably Illinoian, and pre-Illinoian Stages (Weaver, 1992; Swinford and Slucher, 1995).

BELLEFONTAINE OUTLIER

Introduction

The Bellefontaine Outlier is a north-northwest trending highland in eastern Logan and northern Champaign Counties in west-central Ohio. Despite extensive glaciation, the Outlier rises 500 ft above the surrounding terrain. Its topographically high Devonian shales lie about 25 miles from the next closest outcrop of similar Devonian rocks. They are surrounded by older, topographically lower Silurian dolomites. These strata have provided many valuable economic resources including limestone, dolomite, shale, oil, natural gas, and ground water (Swinford and Slucher, 1995).

Stratigraphy

The stratigraphy of the Bellefontaine Outlier Study Area includes the Proterozoic, Paleozoic, and Cenozoic rocks. The majority of the Study Area is underlain by the Proterozoic Granite-Rhyolite Province. Over the Granite-Rhyolite Province Middle Run Fm sandstones and volcanics. In the northeast corner there is a thin wedge of Grenville Province metaigneous, igneous, and metasedimentary rocks. The Paleozoic bedrock includes only Cambrian, Ordovician, Silurian, and Devonian strata. The Cambrian is primarily limestone, dolomite, and sandstone. Ordovician strata includes dolomitic shales and interbedded limestone and shale. The Silurian rocks are argillaceous or shaly dolomites with some limestones and dolomitic shales. The Devonian strata in the Outlier includes dolomites and carbonaceous shales and concretions. On the surface is a thick cover of Quaternary glacial drift and alluvium (Figure 3) (Swinford and Slucher, 1995; Janssens, 1973).

The bedrock formations' areal distribution is controlled by former Teays River's (Pleistocene or older) erosion of the bedrock surface. The Teays and its tributaries are oriented northeast and northwest, the same as the fault trends in this study. Capping the Outlier are Pleistocene and Holocene drift and alluvium ranging from 0-250+ ft thick (Swinford and Slucher, 1995).

Structure

The Bellefontaine Outlier has previously been interpreted as an erosional remnant from the most recent, Wisconsin Stage, glaciation. Recent evidence from the COCORP OH-1 seismic line has resulted in an interpretation of the Outlier as a reverse graben. That is, instead of being surrounded by normal faults, high-angle reverse faults enclose the down-dropped block, surrounding Devonian strata with older Silurian rocks. The Outlier is situated on the northeast edge of the Cincinnati Arch. It is south of the Findlay Arch between the Appalachian, Illinois, and Michigan Basins, and lies within the Fort Wayne Rift (Weaver, 1992).

The Outlier is located over the zone of thrust faulted basement rocks, the Grenville Front Tectonic Zone (Fig. 3). The reprocessed COCORP Seismic Line OH-1 shows east-dipping layered rocks lying over a footwall ramp of the Grenville Front. The Precambrian faults are thought to have influenced the structural and stratigraphic history of the overlying Phanerozoic sediments (Wickstrom et al., 1992). The weakened basement rocks would be prone to reactivation with increased stress. The Auglaize, Logan-Hardin, Bowling Green, and Union Faults may be expressions of such reactivation (Wickstrom, 1990). In the COCORP line, a series of deep-seated, high-angle faults cut up through the Paleozoic section to the highest parts of the Outlier. This is an indication of the close structural relationship between the Outlier and the deep structural basement complex (Drahovzal et al. 1992).

GRAVITY PROFILES

Introduction

The basement structure and topography in Figure 5 are from the work of the Indiana, Kentucky, and Ohio Geological Surveys in the Cincinnati Arch Consortium, much of which is published in Drahovzal et al. (1992). The topographic, gravity, and station location data are directly from Weaver, (1992) who gathered the data and performed the preliminary analysis (Figures 6 and 7).

The Complete Bouguer Residual Anomaly data as calculated by Weaver (1992) are more detailed than that of previous studies because of the greater number of stations in a much tighter area (Figure 8). This information was used to check the locations and throws of the faults in (Figure 5) Drahovzal et al. (1992). Profiles were to be constructed approximately perpendicular to these faults. It was found, however, that the fault trends did not always coincide with the trends observed in the gravity data. Therefore, the profiles in this study were located (Figures 9-11) using Weaver's data, rather than trying to follow the faults in Drahovzal et al. (1992). Fault locations and throws were calculated and the results compared with the structure map.

Methods

Some basic assumptions were made concerning the nature of the Bellefontaine Outlier's structure and stratigraphy. For simplicity in the fault throw calculations, all faults were considered vertical or near vertical. Of the strata above the crystalline basement, the majority is Middle Run Formation clastics and volcanics. This unit has the greatest effect on the gravity, so it is the main factor in the overburden density.

Profiles of the Complete Bouguer Residual Anomaly were chosen to minimize their number while representing the most salient features within the area. Initially, they were intended to be approximately perpendicular to the faults interpreted in Drahovzal et al. (1992) (Figure 5). They have a regular northwest-southeast and northeast-southwest trend. Inspection of the gravity data (Figure 7), however, shows the trend within the Study Area to be oriented somewhat more north-south. Consequently, the profiles were constructed perpendicular to the trend of the gravity (and consequently perpendicular to the

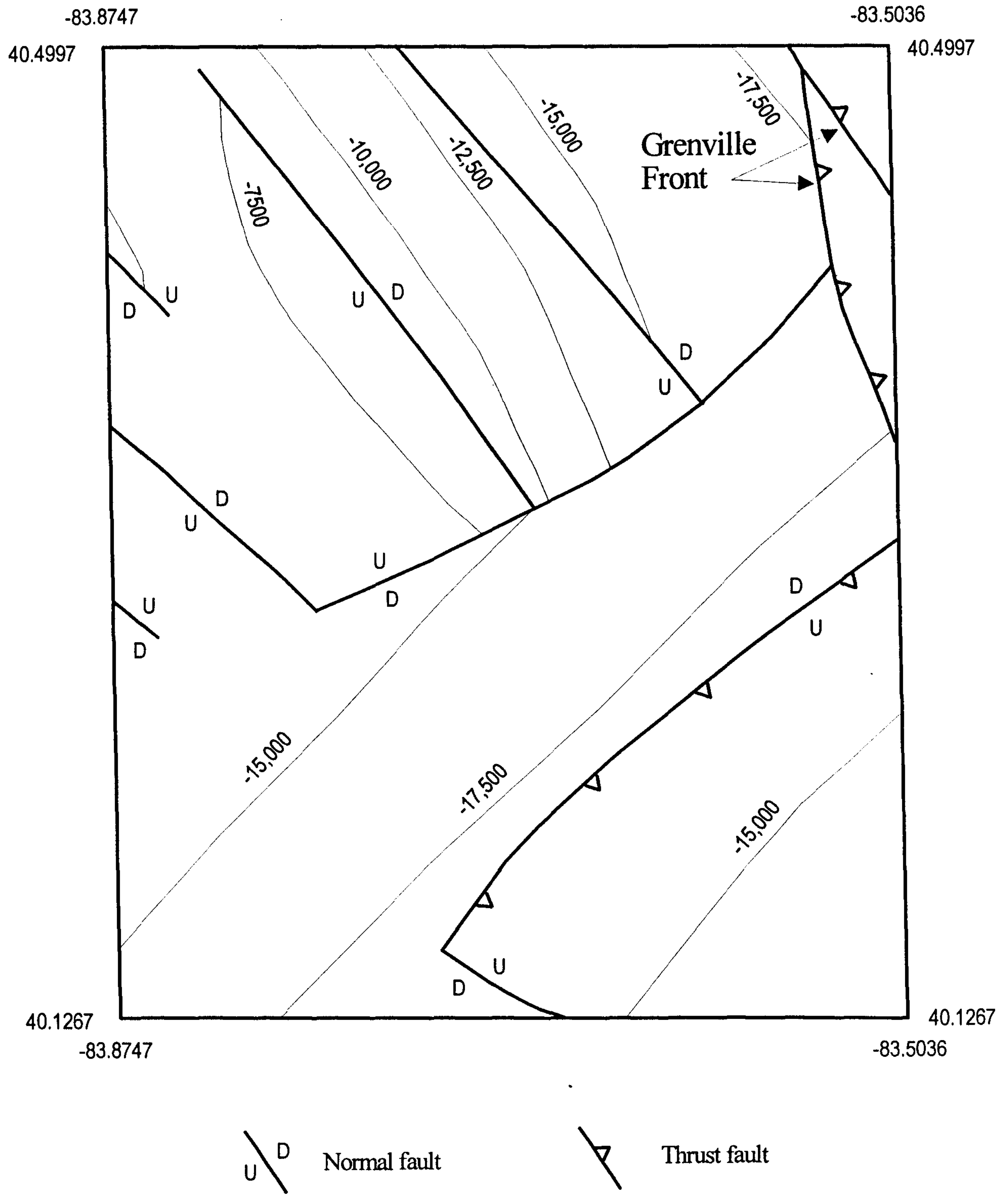

Figure 5. Structure contour map of the Precambrian crystalline basement surface in the Study Area. Contour Interval is 2,500 ft. All depths below mean sea level. Modified from Wickstrom et al., 1992.

Figure 6. Topography of the Bellefontaine Outlier Study Area. Contour Interval is 50 ft. Modified from Weaver, 1992.

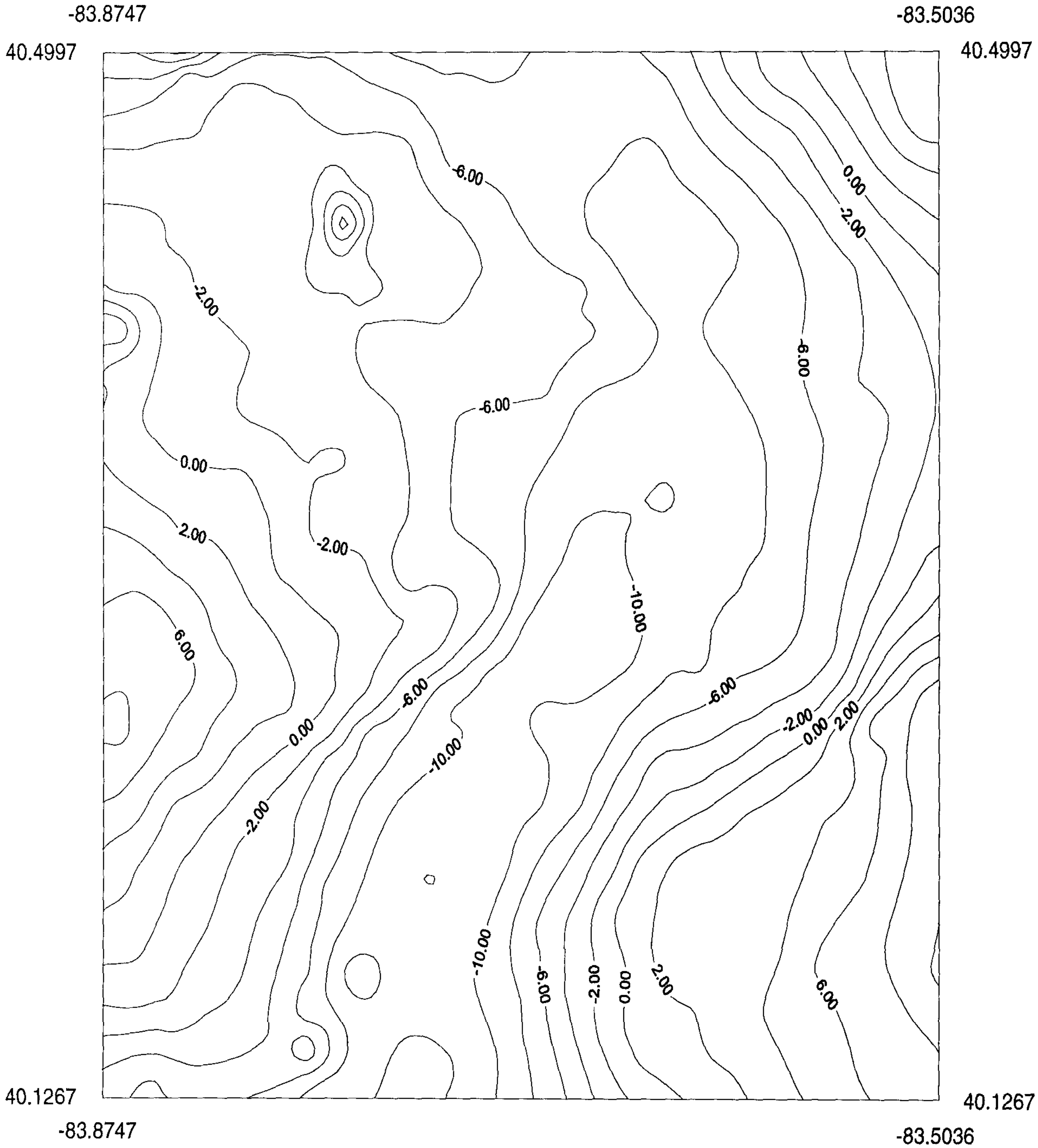

Figure 7. Complete Bouguer Residual Anomaly in the Study Area. Contour interval is mgal. Modified from Weaver, 1992.

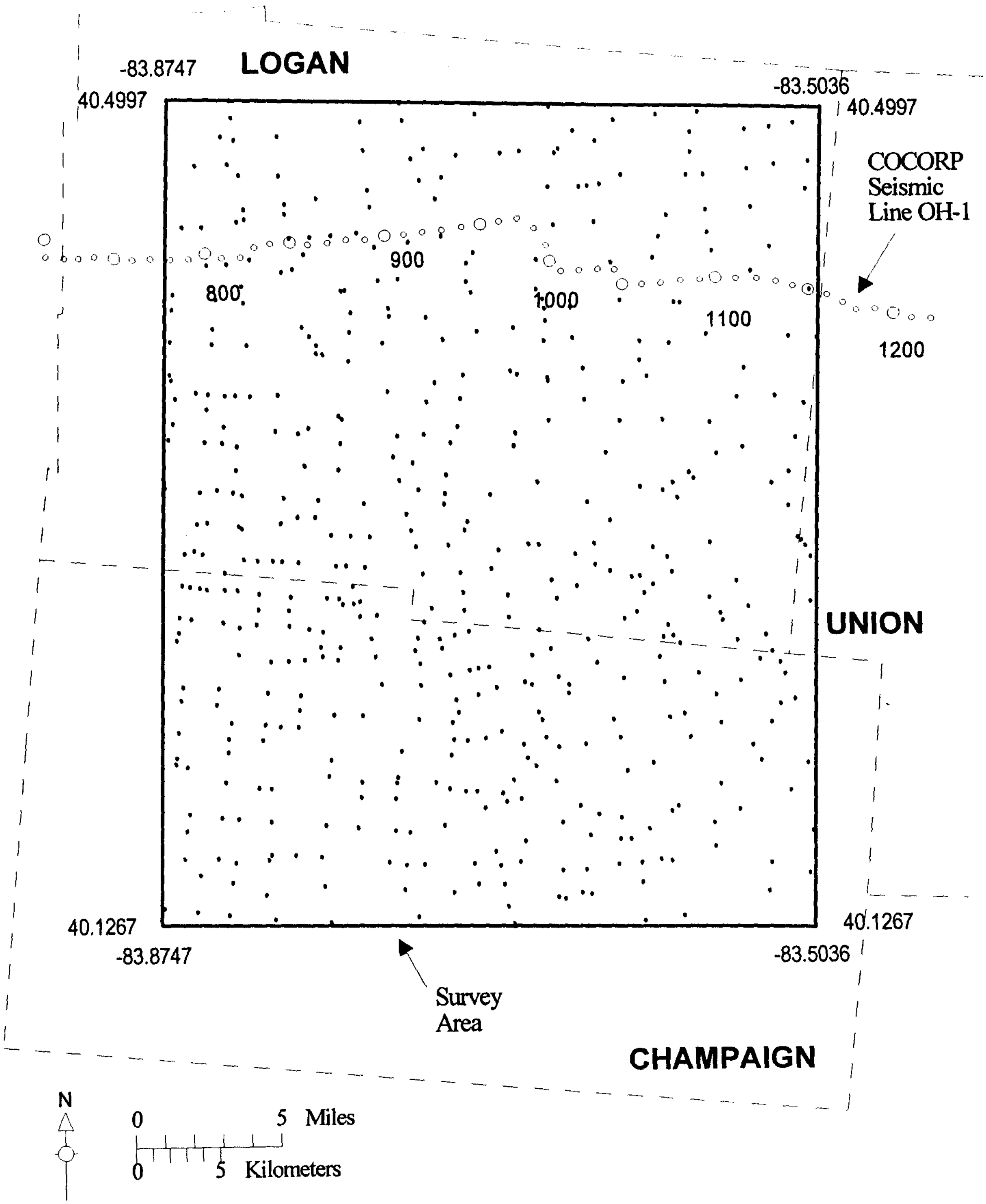

Figure 8. Station locations (510) in the Bellefontaine Outlier Study Area, modified from Weaver (1992).

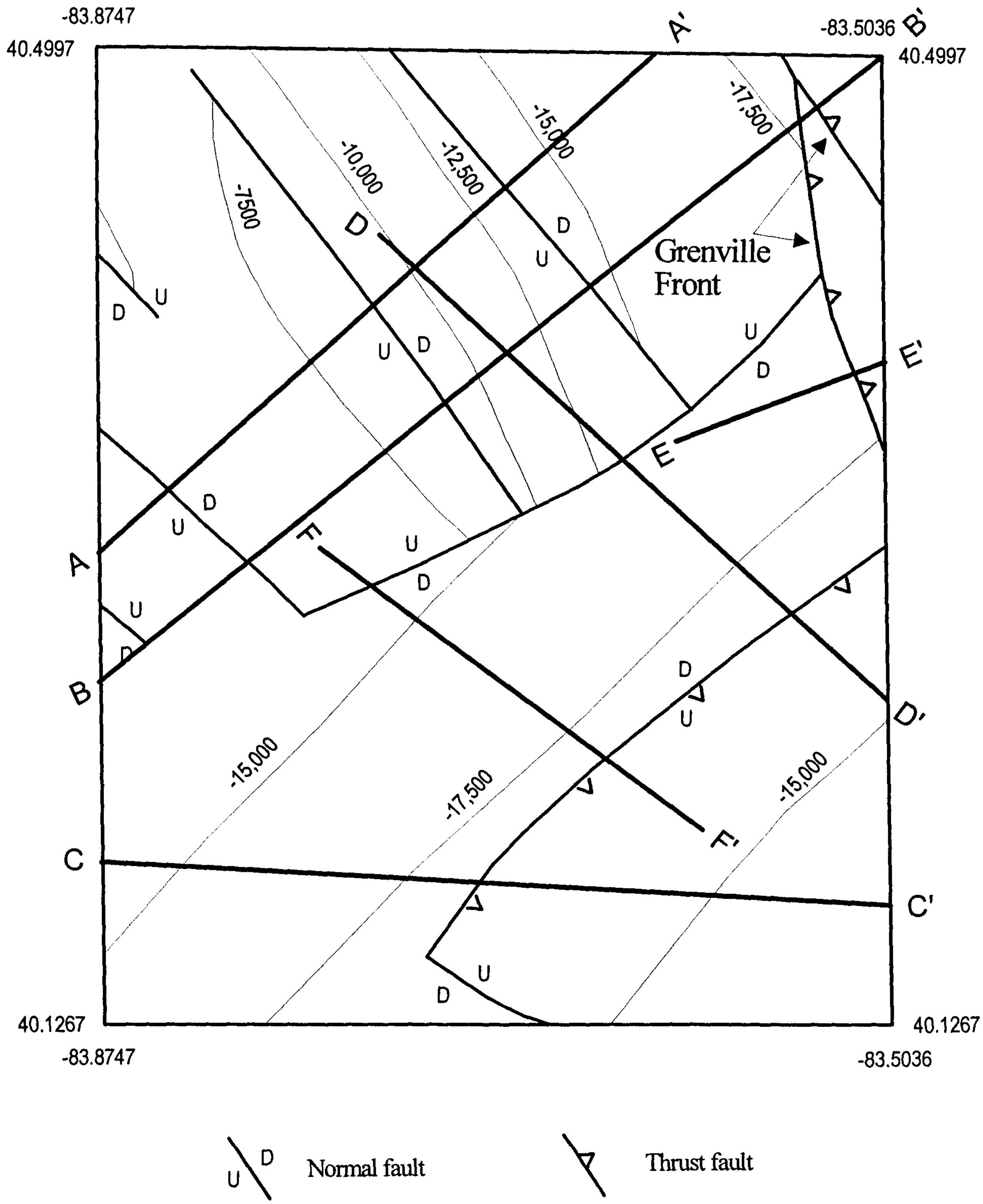

Figure 9. Structure contour map of the Precambrian crystalline basement surface in the Study Area with profile locations. Contour Interval is 2,500 ft. All depths below mean sea leve. Modified from Wickstrom et al, 1992.

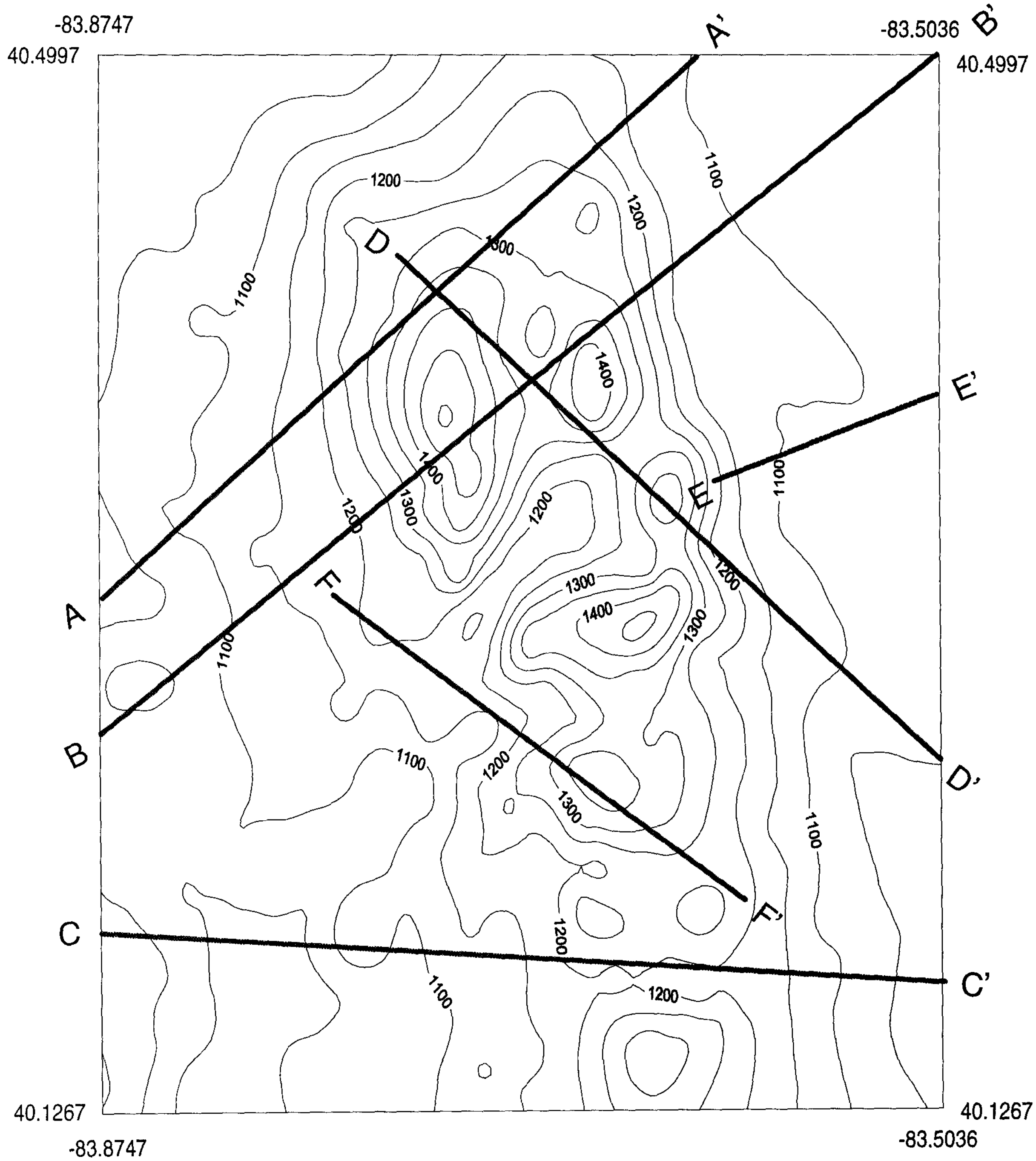

Figure 10. Topography of the Bellefontaine Outlier Study Area with profile locations. Contour Interval is 50 ft. Modified from Weaver (1992).

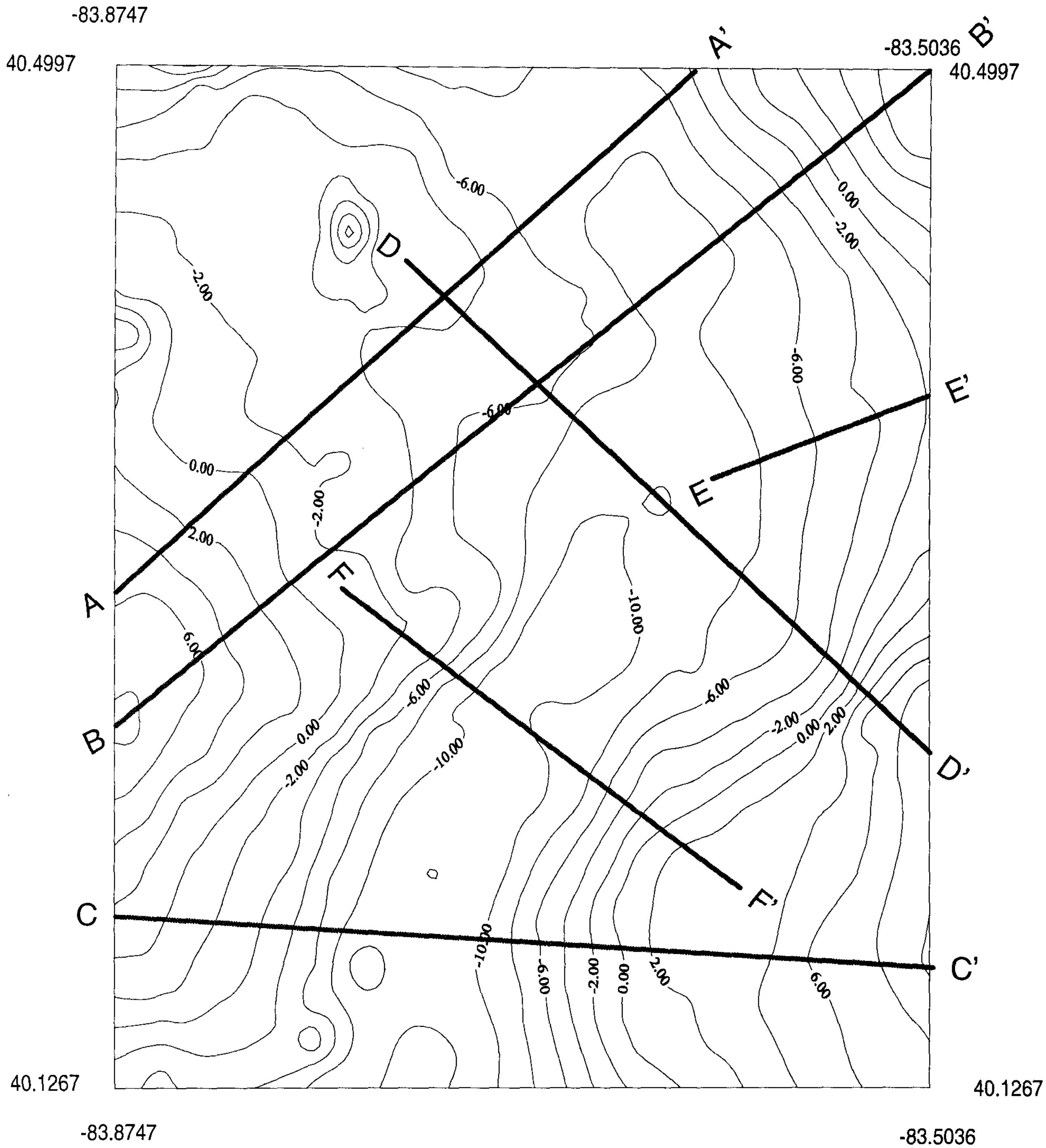

Figure 11. Complete Bouguer Residual Anomaly map of the Bellefontaine Outlier Study Area with profile locations. Contour Interval is mgal. Modified from Wickstrom et al., 1992.

faults). The gravity profiles were examined for inflection points, that is, locations where the direction of curvature changed. Because gravity changes fastest directly over the fault, identifying these steepest gradient points on the profile locates the positions of the faults producing the curve. For example, starting on the left side of profile F-F′ and moving from left to right, the gravity is concave down, decreasing from about -1.00 mgal to -6.00 mgals. At -6.00 mgals the curve changes to concave up and decreases more gradually to about -11.00. In this way all the faults in this study were identified.

One goal of this study was to locate the faults in Drahovzal et al. (1992) to better determine their throws and locations. It was hoped that to simplify the calculations, the Thin Slab Approximation (Noltimier, 1996) could be employed:

$$T = \frac{\Delta g}{2\pi G \, \Delta\rho} \qquad \text{(Eqn. 1)}$$

where:

T = throw of the fault

Δg = change in gravity across the fault

G = universal gravitational constant

$\Delta\rho$ = change in density across the fault

This is a simple and direct relationship between the fault's throw and the change in gravity and material density across the fault. The method assumes, however, that the throw of the fault is on the order of ten percent or less of the mean depth to the fault. Direct calculations from the basement structure contour map (Figure 5) of the major fault throws versus depth to basement show that this is not the case. Many of the fault throws are in excess of fifty or sixty percent of their average depth. Some, in fact, appear to extend to the highest elevations of the Bellefontaine Outlier based on the reprocessed COCORP OH-1 Seismic Line (Drahovzal et al., 1992). Consequently, a more complex equation (Eqn. 2) was used that is not dependent on mean fault depth. This equation relates the rate of change of gravity and density across the fault and the upper and lower depths of the fault (Noltimier, 1996).

$$\frac{d}{dy}\left(\Delta g_z\right) = G \, \Delta\rho \, \ln\left(\frac{z_1^2}{z_0^2}\right) \qquad \text{(Eqn. 2)}$$

where

$\frac{d}{dy}(\Delta g_z)$ = rate of change in gravity across the fault

G = universal gravitational constant

$\Delta\rho$ = change in density across the fault

z_1 = deepest part of the fault surface

z_0 = shallowest part of the fault surface

Another goal of this study was to locate any additional faults not recognized in Drahovzal et al. (1992). The locations of portions the faults located do not coincide with those of the previous study. These are probably the same faults appearing in a more correct position, but they may in some cases represent newly recognized faults or faults zones not recognized by Drahovzal et al. (1992).

<u>Sample Calculation</u>

The following is a sample calculation for the throw and location of fault D-2 based on Equation 2. The value for the Universal Gravity Constant used was $6.67*10^{-8}$ dyne$\times$cm^2/gm^2 (Telford et al., 1976). The thicknesses and densities of the bedrock above the Middle Run Formation are from Weaver (1992). These layers were determined to have the greatest effect on the gravity gradient in the Study Area (Table 1). The combined effect of the densities of the overburden above the Middle Run Fm. (2.68 gm/cm^3) and the Middle Run Formation clastics and volcanics (2.58 gm/cm^3) was calculated to be 2.59 gm/cm^3. A value of 2.65 gm/cm^3 was used for the crystalline basement (assumed to be in the Granite-Rhyolite Province). Only one deep well in the Study Area has penetrated crystalline basement and was determined from cuttings to be rhyolite. The cuttings of other wells just outside the Study Area to the west and the south were found to have penetrated gabbro and/or basalt. The closest well in the Grenville Province just outside the northeast corner of the Study Area contained schist. The change in density between the basement and bedrock was 0.06 gm/cm^3.

Table 1

All major units, thicknesses, and densities used for the throw calculations. These have the most significant influence on the gravity anomalies. Because the thickness of the Middle Run Fm. is highly variable within the Study Area, densities for the thickest and thinnest parts of the total overburden are given. For units above the Middle Run Fm., values are from Weaver (1992). Middle Run Fm. thicknesses are from Drahovzal et al. (1992). Density values for the Middle Run Fm. and the crystalline basement are from Telford et al. (1976).

Unit	Thickness (feet)	% of column	Average density (gm/cc)	Weighted density (gm/cc)
Overburden with thinnest Middle Run Fm.				
Quaternary drift & alluvium	79	1.31	2.00	0.03
Ohio Shale	105	1.75	2.67	0.05
Salina undif.	136	2.26	2.78	0.06
Knox Dolomite	394	6.55	2.84	0.19
Eau Claire Fm.	178	2.96	2.71	0.08
Mt. Simon Ss.	120	2.00	2.42	0.05
Middle Run Formation	5000	83.17	2.58	2.15
Total:	6012	100.00		2.60
Overburden with thickest Middle Run Fm.				
Quaternary drift & alluvium	79	0.45	2.00	0.01
Ohio Shale	105	0.60	2.67	0.02
Salina undif.	136	0.78	2.78	0.02
Knox Dolomite	394	2.25	2.84	0.06
Eau Claire Fm.	178	1.02	2.71	0.03
Mt. Simon Ss.	120	0.69	2.42	0.02
Middle Run Formation	16500	94.22	2.58	2.43
Total:	17512	100.00		2.59
Crystalline Basement				
Granite-Rhyolite Province	-	-	2.65	2.65
Grenville Province	-	-	2.70	2.70

The gravity profile was constructed and faults were identified based on where the gradient was steepest. On either side of the fault, the highest and lowest gravity values and locations were noted. The change across the fault was computed from the gravity, latitude and longitude values. The latitude and longitude were measured in decimal degrees, but must be converted to centimeters for the calculation. One degree of latitude equals $1.11*10^8$ cm, so

$40.2500(1.11*10^8) - 40.3475(1.11*10^8) = -1.0823*10^7$ cm,

the distance from the change in latitude.

One degree of longitude equals $1°\cos\phi(1.11*10^8)$ cm, where ϕ is latitude, so

$(\cos 40.2500 - \cos 40.3475)1.11*10^8 = 5.5802*10^7$ cm,

the distance from the change in longitude.

Change in gravity: 19.3013 mgal. For the calculation this value needs converted to: $1.93013*10^{-2}$ Gal. The following equation (Eqn. 3) was used to calculate the distance across the fault.

$$\sqrt{\Delta\phi^2 + \Delta\psi^2} = 5.6841*10^7 \text{ cm} \qquad \text{(Eqn. 3)}$$

where

$\Delta\phi$ = the change in latitude (cm)

$\Delta\psi$ = the change in longitude (cm)

This distance is divided by the change in gravity to obtain the rate of change in gravity across the fault,

$$\frac{d}{dy}(\Delta g_z) = 3.3956*10^{-10} \text{ Gal/cm} \qquad \text{(Eqn. 4)}$$

where

Δg_z = the vertical change in gravity (Gal) across the fault.

Now, rearranging Eqn. 2 for the ratio of the deepest to the shallowest part of the fault surface, we obtain:

$$\frac{z_1}{z_0} = \sqrt{e \ \exp\left[\frac{d}{dy}(\Delta g_z) \Big/ G\,\Delta\rho\right]} = 1.0416 \qquad \text{(Eqn. 5)}$$

All calculations to this point have used the gravity data in Weaver (1992). Depths to the upper and lower edges of the fault surfaces from Figure 5 (Drahovzal et al., 1992) are subtracted to obtain the actual throw:

Throw from Figure 5 map: -13,700 - (-18,400) = 4700 ft

Dividing these depths gives a ratio of 1.3431, which is compared to the ratio calculated from Weaver's (1992) gravity data. Multiplying the throw calculated from Figure 5 by my calculated ratio and dividing by the ratio from Figure 5 gives the throw suggested by my gravity data.

4700 * 1.0416 / 1.3431 = 3645 ft

This yields a difference between the throw calculated here and from Figure 5 of 1055 ft. This is 22% less than the throw indicated on the Figure 5 map, which is about average for the faults in this study. Based on the gravity profile, the location of this fault is about 2754 ft from the point on the Figure 5 map. Relative to the other faults in this study, the agreement in location is better than average (Table 2).

To test the result of the throw calculation, which depends upon my measurement of the lateral gravity gradient, the ratio of the change in gravity to the change in lateral distance across the fault was increased by five percent. This did not result in any significant change in the calculated value of z_1/z_0. The new z_1/z_0 ratio was only about 0.41% higher with the increased lateral gravity gradient (Table 3).

Results

The major faults shown on the Precambrian crystalline basement map in Figure 5 (Drahovzal et al., 1992) were recognized in the gravity profiles from this study (cf. Figure 18). They all retained the same sense of displacement but the locations and throws have been modified here. The lengths of some faults were extended, while other faults were not clearly seen in the gravity data and were discarded.

In profile Figures 12-17, the top graph represents the present day surface topography. The middle graph is the Complete Bouguer Residual Anomaly. The bottom graph is the inferred Precambrian crystalline basement structure which has the greatest effect on the gravity. No scale is implied for the basement structure, only the sense of displacement and relative magnitudes of motion. A comparison of the calculated locations and throws in this study compared with Drahovzal et al. (1992) is summarized in Table 2.

Table 2

Thickness and density of the overburden, change in density and distance across the faults, top-of-fault to bottom-of-fault ratios, calculated throws, throw differences, and location differences for the Bellefontaine Outlier Study Area.

A	B	C	D	E	F	G	H	I	J	K	L	M	N
Fault	Middle Run Fm. thickness (feet)	Middle Run Fm. density (gm/cc)	Total Over-burden thickness (feet)	Total Over-burden density (gm/cc)	Change in density (gm/cc)	Distance across fault (cm)	Throw (feet) (from Fig. 5)	z1 / z0 (from Fig. 5)	Throw (feet) calculated	z1 / z0 calculated	Throw difference (feet)	Throw difference (%)	Distance between faults (feet)
A-1	5000	2.58	6012	2.60	0.05	4.3461E+07	250	1.0250	251	1.0308	-1	0.6	4590
A-2	7500	2.58	8512	2.59	0.06	3.5512E+07	1000	1.0755	941	1.0125	59	-5.9	17378
B-1	5000	2.58	6012	2.60	0.05	5.6375E+07	500	1.0400	498	1.0366	2	-0.3	2295
B-2	7500	2.58	8512	2.59	0.06	3.0021E+07	750	1.0536	722	1.0149	28	-3.7	1836
B-3	15000	2.58	16012	2.59	0.11	3.2372E+07	15475	8.6420	1855	1.0356	13620	-88.0	7345
C-1	13000	2.58	14012	2.59	0.06	4.9980E+06	-	-	-	1.3645	-	-	-
C-2	12000	2.58	13012	2.59	0.06	5.1136E+06	5250	1.4038	5241	1.4013	9	-0.2	14689
D-1	10000	2.58	11012	2.59	0.06	4.1017E+07	3000	1.2400	2471	1.0215	529	-17.6	37707
D-2	12500	2.58	13512	2.59	0.06	5.6841E+07	4700	1.3431	3645	1.0416	1055	-22.4	2754
E-1	15000	2.58	16012	2.59	0.06	1.5609E+07	-	-	-	1.0576	-	-	-
F-1	10000	2.58	11012	2.59	0.06	3.0392E+07	3000	1.2727	2446	1.0376	554	-18.5	14099
F-2	16500	2.58	17512	2.59	0.06	3.5828E+07	4750	1.3585	3647	1.0430	1103	-23.2	0

Key	
A	Letter indicates profile, number indicates fault.
B	Thickness of Middle Run Fm. (feet).
C	Density of Middle Run Fm. (gm/cc).
D	Thickness of Total Overburden (feet).
E	Density of Total Overburden (gm/cc).
F	Change in density across the fault (gm/cc).
G	Distance across the fault used for calculation (cm).
H	Throw of fault calculated from Figure 5 (feet).
I	Top-of-fault to bottom-of-fault ratio calculated from Figure 5.
J	Throw of fault calculated from gravity data (feet).
K	Top-of-fault to bottom-of-fault ratio calculated from gravity data.
L	Throw difference between calculated and Figure 5 (feet).
M	Throw difference between calculated and Figure 5 (%).
N	Distance (feet) between faults in Figure 5 (Drahovzal et al., 1992) and Figure 18 (this study).

Table 3

A 5% increase in the change-in-gravity to change-in-distance ratio across the faults. Results on average increase about 0.41% the ratio of z_1/z_0, the deepest to shallowest parts of the fault.

A	B	C	D	E
Fault	Chg. in grav to chg. in dist. plus 5%	zl / z0 plus 5%	Original zl / z0	zl/z0 difference (%)
A-1	2.2594E-10	1.0324	1.0308	0.1518
A-2	1.0127E-10	1.0131	1.0125	0.0622
B-1	2.6760E-10	1.0385	1.0366	0.1798
B-2	1.2070E-10	1.0157	1.0149	0.0742
B-3	5.5770E-10	1.0375	1.0356	0.1753
C-1	2.7327E-09	1.3858	1.3645	1.5660
C-2	2.9409E-09	1.4252	1.4013	1.7015
D-1	1.8120E-10	1.0226	1.0215	0.1064
D-2	3.5654E-10	1.0437	1.0416	0.2038
E-1	4.9916E-10	1.0605	1.0576	0.2802
F-1	3.1479E-10	1.0396	1.0376	0.1850
F-2	3.7905E-10	1.0452	1.0430	0.2109
		Mean % change		0.4081

Key

A Letter indicates profile, number indicates fault.
B 5% increase in the ratio of change in gravity to change in distance across the fault.
C Top-of-fault to bottom-of-fault ratio with the 5% increase in B.
D Top-of-fault to bottom-of-fault ratio without the 5% increase in B.
E Percentage change between original ratio and ratio with 5% increase in B.

Profile A (Figure 12)

Two significant faults were recognized in Profile A . A third appears to be just outside the Study Area to the northeast. Fault A-1 is up to the west, and causes a change in gravity of about nine milligals. Its location in Figure 18 was based on the location of fault B-1 (Figure 13) and the steep northwest gravity trend in this vicinity (Figure 11). This fault corresponds with the northwest trending fault in the west-central portion of Figure 5. While the fault's location varies up to 5000 ft, the throws agree within one percent. Fault A-2 corresponds to the northwest trending fault in the same location in Figure 5. While it is much more sinuous and lies farther to the west than the later fault, the calculated throw is only about six percent less. Fault A-3 does not appear on the map in Figure 18. It is thought to lie to the northeast of the Study Area. It is displaced up to the east like B-3 and appears to be the extension of that fault. A-3 and B-3 roughly correspond to the Grenville Front in Figure 5. The location of A-3 was determined in the same way as A-2: using B-3's location and the northwest gravity trend.

Profile B (Figure 13)

The gravity profile indicates the displacement of faults B-1 and B-2 are up to the west, as in Figure 5. A-1 and B-1 appear to be the same fault. B-2 lies only about 1800 ft from its place in Figure 5. A-2 and B-2 also appear to be connected, but not as the two faults in Figure 5 indicate. This fault is not as segmented as the corresponding fault in Figure 5, and is may be a composite of many smaller faults. Fault B-3 has a large gravity gradient (~ 17 mgal) showing it to be up to the east. The gravity data used in this study shows only one fault at this location, but Figure 5 shows two, interpreted to be a splay of the Grenville Front. Based on my gravity data alone, it is not possible to determine the attitude of this fault, therefore I am indicating only which side of this fault is higher.

Profile C (Figure 14)

There are two large faults in Profile C. Fault C-1is up to the west and C-2 is up to the east. They form the southern end of the prominent graben in the Study Area. The northeast-southwest trending fault in the center of Figure 5 does not extend into this area (Figure 18). Because there is no corresponding fault

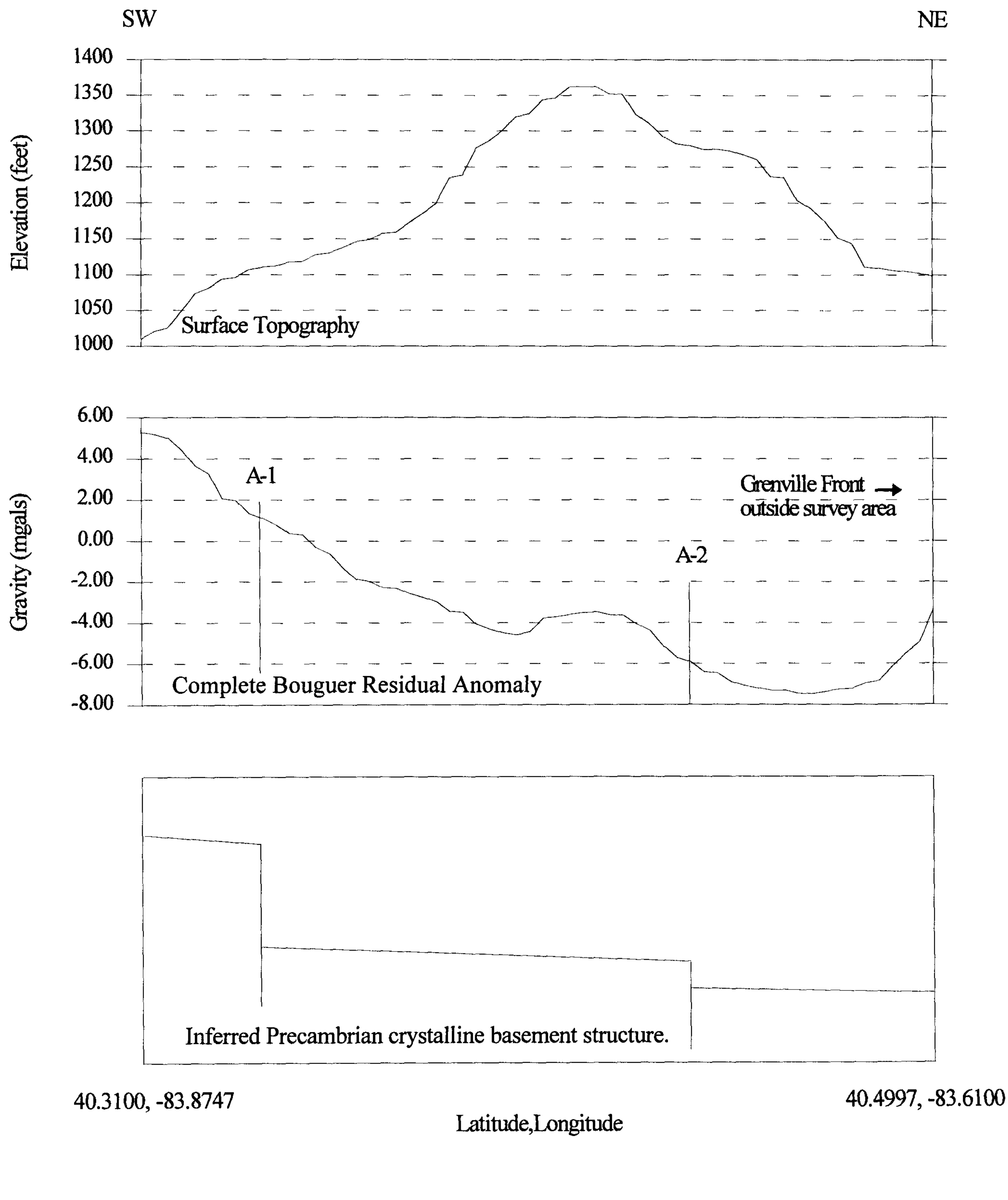

Figure 12. Profile A-A' Topography, gravity, and basement structure

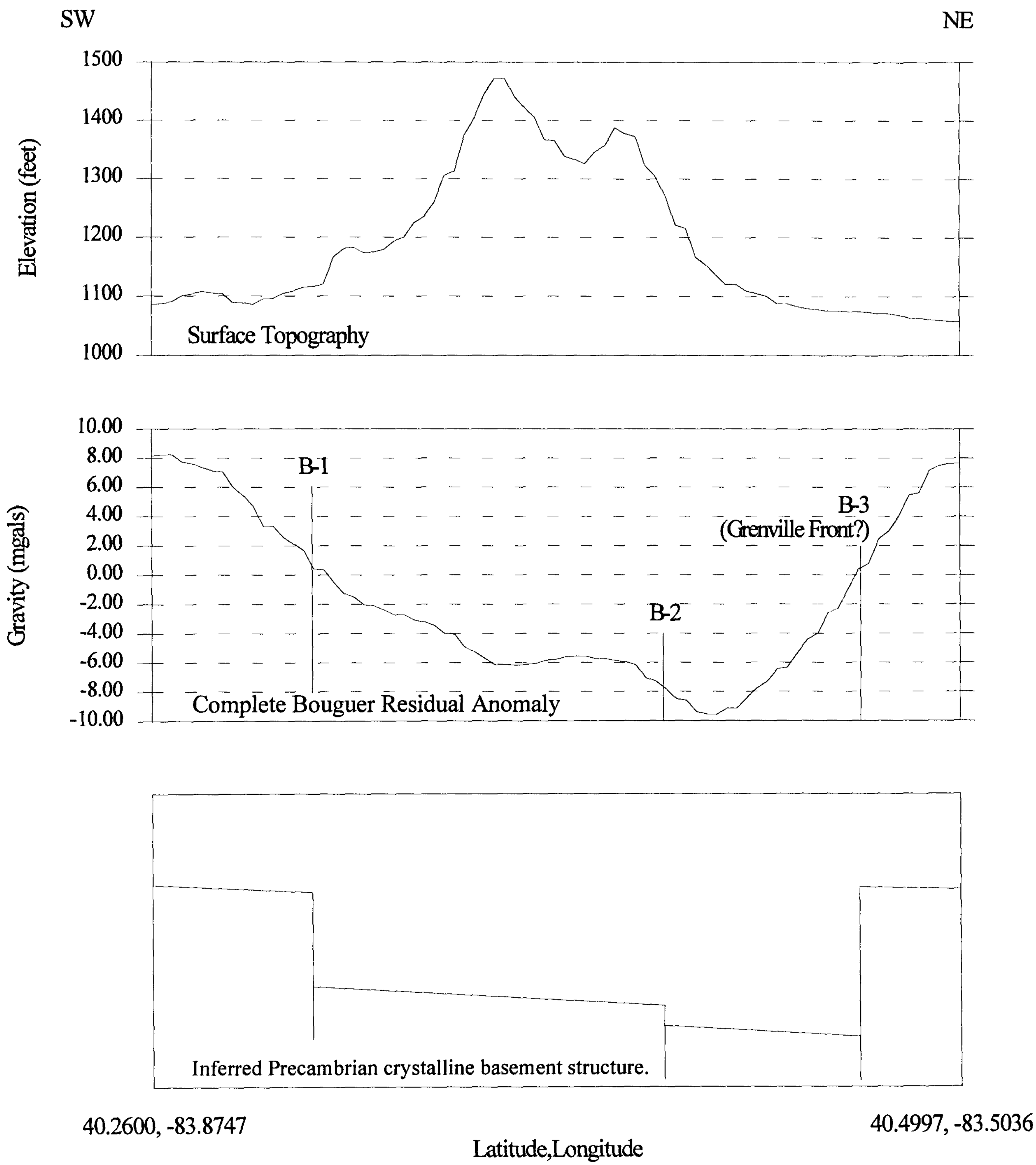

Figure 13. Profile B-B' Topography, gravity, and basement structure

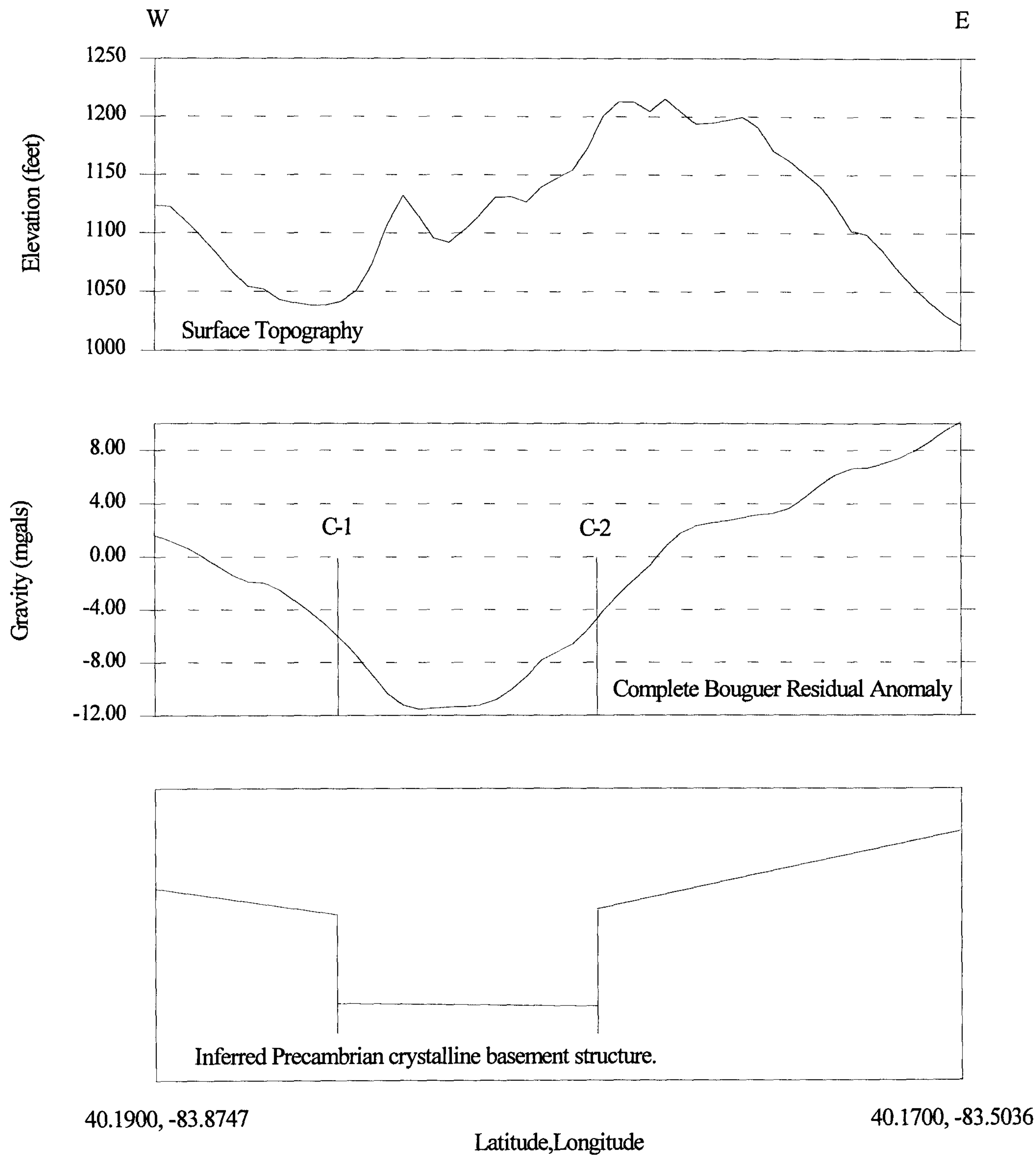

Figure 14. Profile C-C' Topography, gravity, and basement structure

at this point, the throw can not be determined, only the location. Fault C-2, on the eastern side of the graben, coincides with the fault in Figure 5, and is not as segmented. Without reference to Figure 4, this fault could be interpreted as an extension of fault B-3. However, the acute angle of intersection they make if projected using Figure 18 makes it more likely that this fault is truncated by fault B-3, which agrees with Figure 4.

Profile D (Figure 15)

Profile D shows one small fault (up to the northwest) and a much larger fault (up to the southeast) that transect the large graben in the Study Area (Figure 18). The location of D-1 does not match the fault in Figure 5 which lies more than six miles to the southeast. It does have the same general trend and sense of displacement, however. The location of Fault D-2 matches well with Figure 5 and appears to be a continuation of faults C-2 and F-2 (Figure 18). The throw, however, is about 22% (1055 ft) less.

Profile E (Figure 16)

Profile E was constructed to better determine whether any fault exists in this area. Figure 5 shows part of the Grenville Front, but the gravity surface (Figure 11) does not appear to level off to the east within the Study Area. Consequently, the fault itself is thought to lie to the east of the position indicated in Figure 5.

Profile F (Figure 17)

The two large faults in Profile F further constrain the location of the graben. Fault F-1is up to the northwest and appears to extend through faults C-1 and D-1. Fault F-2 is up to the southeast and together with D-2 and F-2 form a fault very similar to the one in Figure 5.

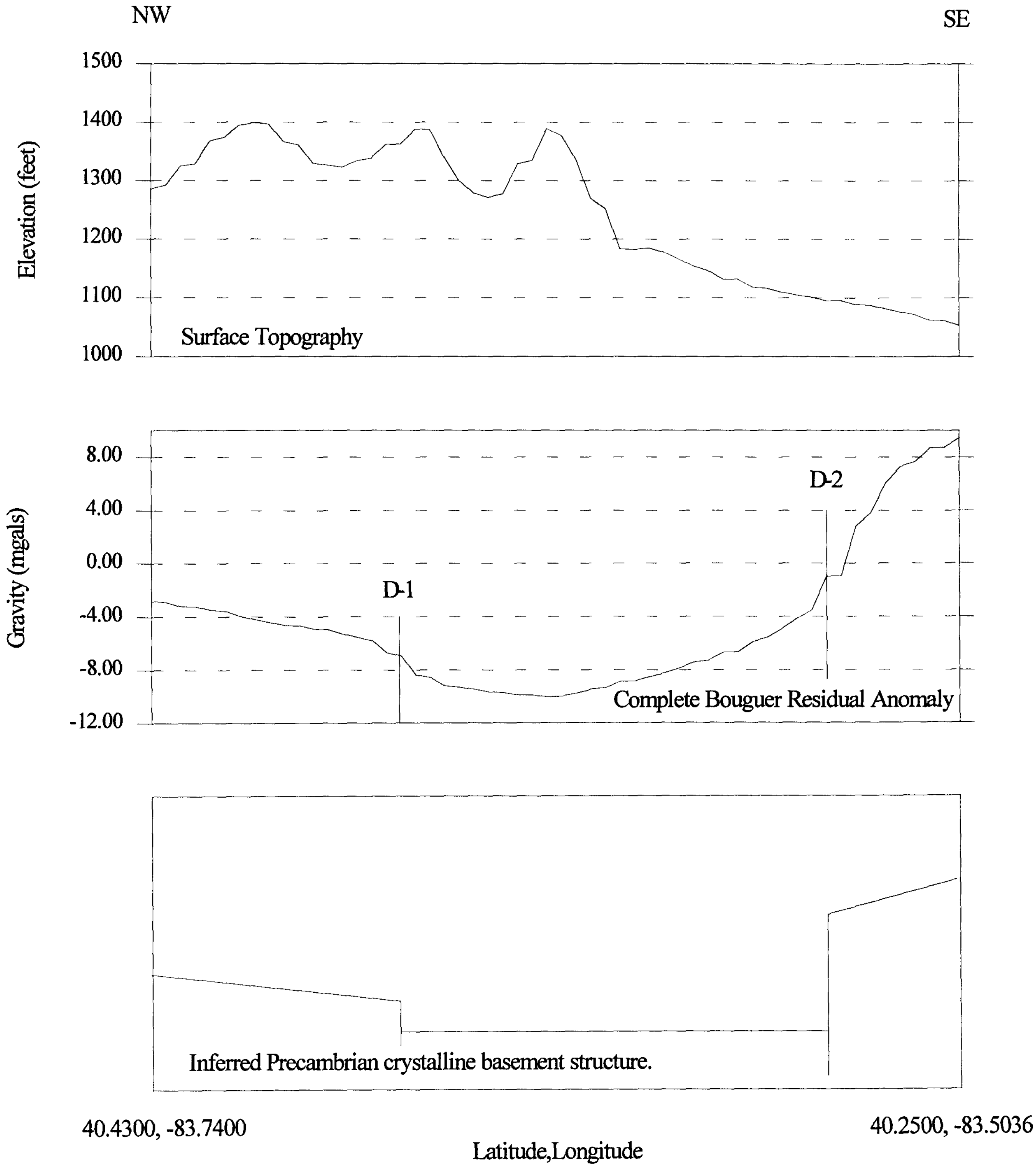

Figure 15. Profile D-D' Topography, gravity, and basement structure

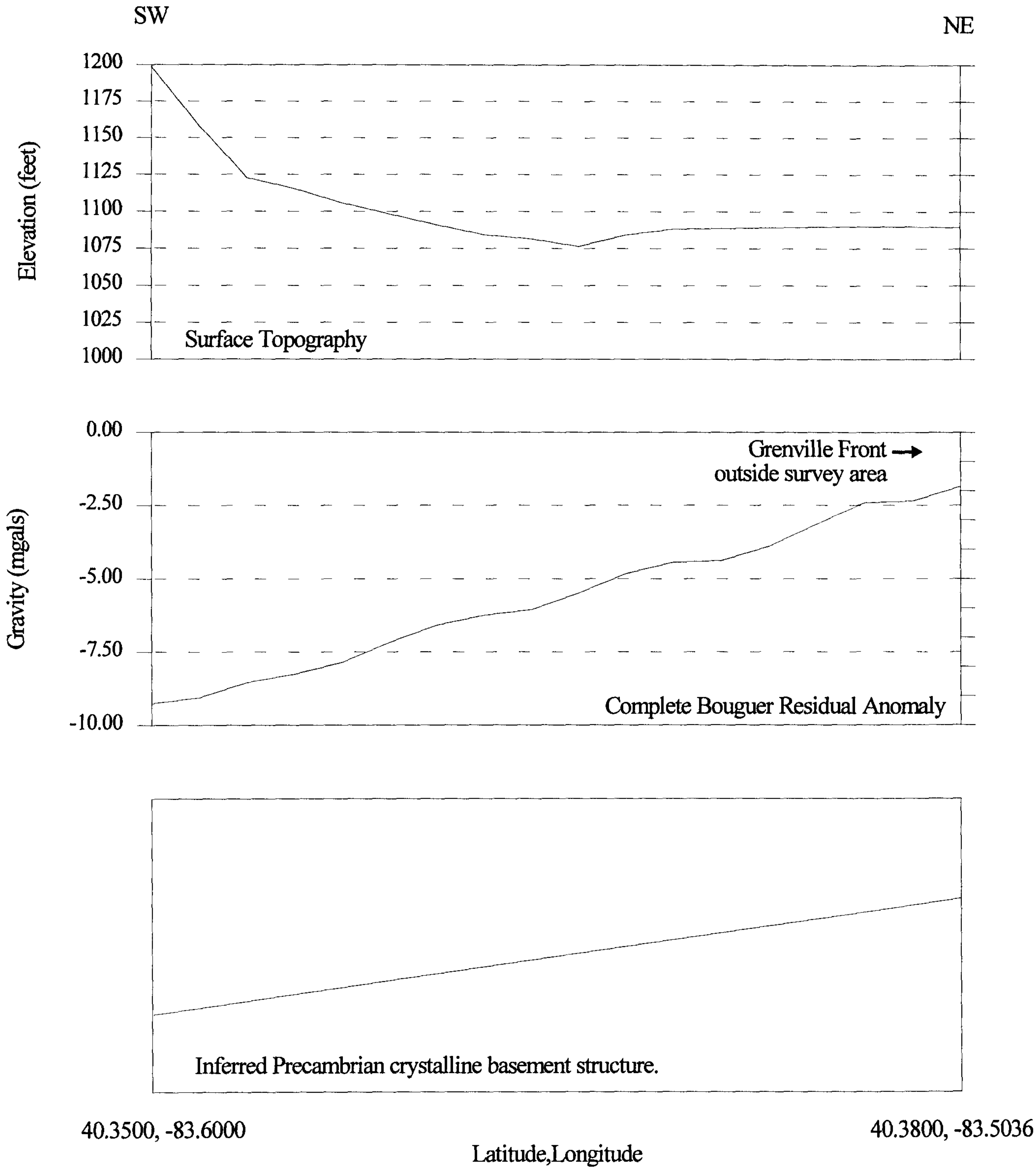

Figure 16. Profile E-E' Topography, gravity, and basement structure

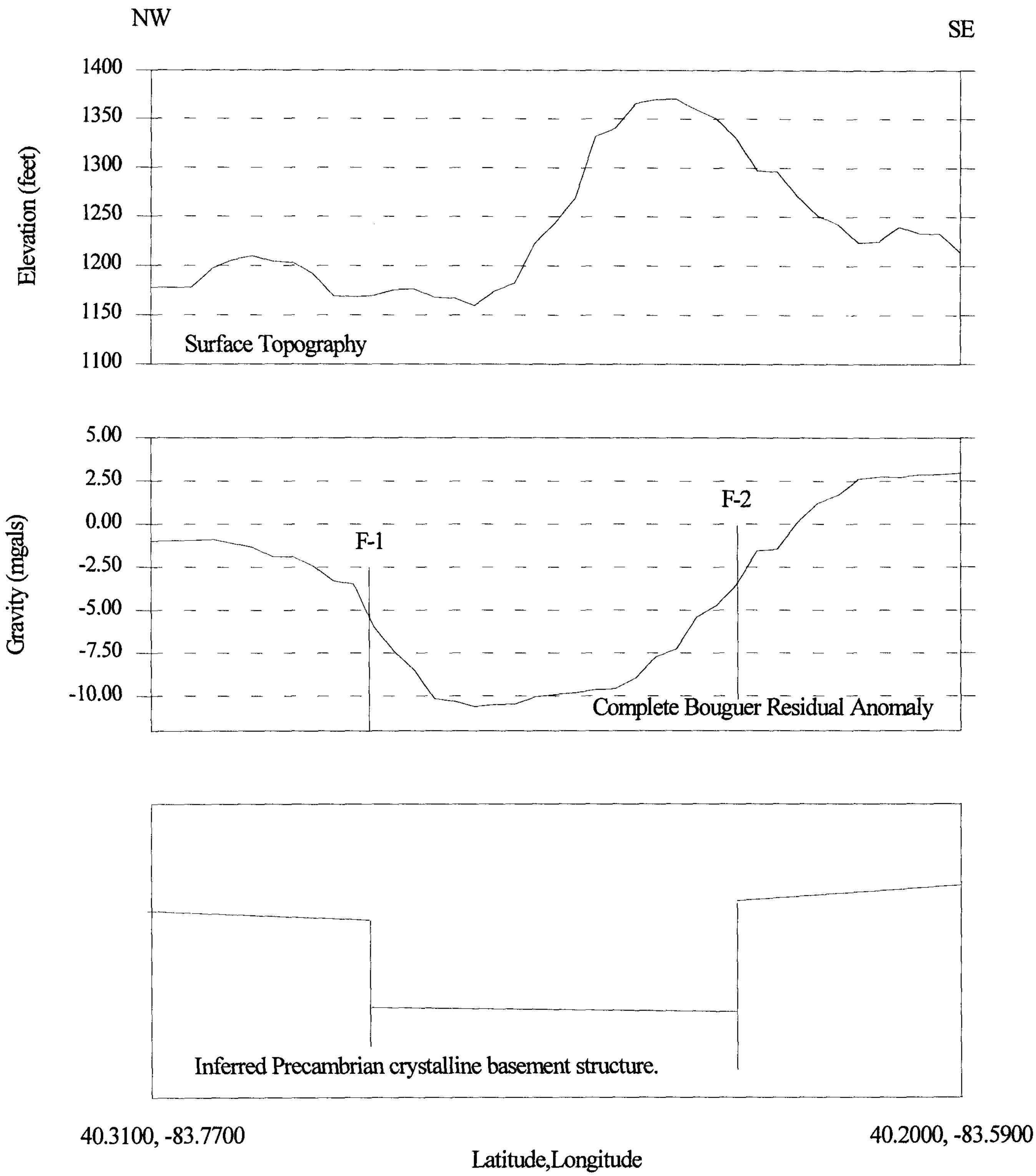

Figure 17. Profile F-F' Topography, gravity, and basement structure

INTERPRETATION AND CONCLUSION

The overall orientations and locations of faults inferred in this study generally matched those in Drahovzal et al. (1992). The northwest and northeast fault trends and the fault throws in the two studies were similar. However, the greater density of the gravity data used here provided additional information resulting in some significant refinements of the prior map. While fewer faults were identified in this study than in Drahovzal et al. (1992), there do appear to be discontinuities in the gravity surface where faults were located in the previous study. No attempt was made to determine the history of movement along these faults, but it is seems reasonable that their motions are consistent with the tectonic history described in Wickstrom et al. (1992) and Drahovzal et al. (1992).

The prominent north-south gravity anomaly in the center of the Study Area is interpreted as a large graben in an open, backwards S shape. All faults were assumed to be near vertical to simplify the throw calculations, but this is not to imply that they are necessarily high-angle normal or reverse, or that the graben is bounded by normal faults dipping toward the center of the structure. In fact, the feature was interpreted to be bounded by reverse faults rather than normal faults in Weaver (1992). Figure 5 from Drahovzal et al. (1992) shows thrust faults on the eastern border. Of the twelve points along the profiles where faults were interpreted to be, ten were analogous to those in Drahovzal et al. (1992). A comparison between Figures 5 and 18 (Table 2) shows that five of those points had throws within six percent of each other. Four were within 17-24 percent. The faults in the central portion had quite variable distances from those in Drahovzal et al. (1992) (Figure 18). On the eastern and western sides of the Study Area, the faults were in generally similar locations and orientations.

Along with the many similarities, some significant differences were noted as well. The structure contours in Figure 5 show the surface in the southwest corner of the Study Area dipping to the southeast, but does not show any fault in this area. Figure 11 shows a very prominent, linear gravity gradient there. In the southeast corner of the Study Area, the contours in Figure 5 show the basement surface uniformly dipping away to the southeast. Again, the gravity in Figure 11 shows that the structure is not as simple. In the northeast corner, Figures 5 and 18 agree on the existence of a fault, but the throw of fault B-3 was

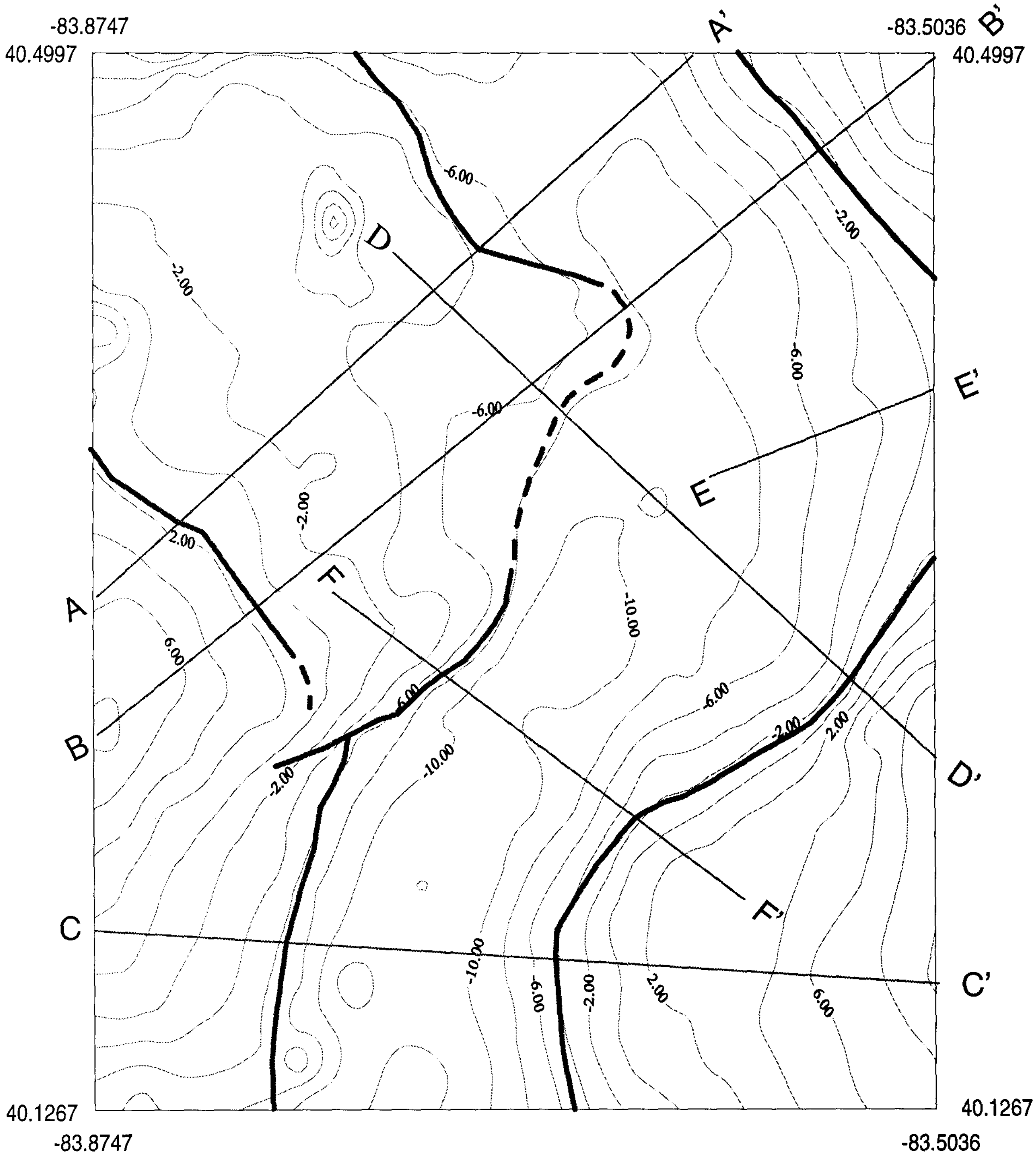

Figure 18. Locations of faults identified in this study. Dashed where inferred.

calculated to be 88 percent less. The fault in Figure 5 is thus approximately eight times larger than what is indicated by the gravity data in this study. Further work is required to resolve this discrepancy.

REFERENCES CITED

Culotta, R. C., T. Pratt, and J. Oliver, A tale of two structures: COCORP's deep seismic surveys of the Grenville province in the eastern U.S. midcontinent, Geology, v. 18, 646-649, 1990.

Drahovzal, J. A., D. C. Harris, L. H. Wickstrom, D. Walker, M. T. Baranoski, B. Keith, and L. C. Furer, The east continent rift basin: a new discovery, Ohio Geol. Surv. Inf. Circ. 57, 1992.

Hansen, M. C., The geology of Ohio—The precambrian, Ohio Geol. Surv. Newsletter, Winter, 1996.

Hull, D. N., Generalized column of bedrock units in Ohio, Ohio Geol. Surv., 1990.

Janssens, A., Stratigraphy of the Cambrian and Lower Ordovician rocks in Ohio, Ohio Geol. Surv. Bull. 64, 197, 1973.

Noltimier, H. C., Geological Sciences 683 course notes, 1996.

Pratt, T., R. Culotta, E. Hauser, D. Nelson, L. Brown, S. Kaufman, and J. Oliver, Major Proterozoic basement features of the eastern midcontinent of North America revealed by recent COCORP profiling, Geology, v. 17, 505-509, 1989).

Stanley, S. M., Exploring earth and life through time, W. H. Freeman and Company, New York, 1993.

Swinford, E. M. and E. R. Slucher, Regional bedrock geology of the Bellefontaine, Ohio, 30 x 60 minute quadrangle, Map no. 8, Ohio Division of Geologic Survey, 1995.

Telford, W. M., L. P. Geldart, R. E. Sheriff, and D. A. Keys, Applied Geophysics, Cambridge University Press, Cambridge, 1976.

Weaver, J. P., A detailed gravity and magnetic survey of the Bellefontaine Outlier, Logan County, Ohio: Master's Thesis, The Ohio State University, 1994.

Wickstrom, L. H., A new look at Trenton (Ordovician) structure in northwestern Ohio, Northeastern Geology, v. 12, no. 3, 103-113, 1990.

Wickstrom, L. H., J. A. Drahovzal, B. D. Keith, Coordinators, The geology and geophysics of the east continent rift basin: Indiana Geological Survey Open File Report OFR92-4, 1992.

Appendix

List of Gravity and Elevation Data. Includes the latitude, longitude, gravity, and surface elevation values for all stations (510) in the Study Area, from Weaver (1992).

Appendix continued

Latitude	Longitude	CBRA (mgal)	Elevation (feet)
40.1267	-83.6328	-1.31	1287
40.1278	-83.6744	-6.95	1152
40.1281	-83.7792	-11.72	1070
40.1292	-83.6000	0.93	1219
40.1294	-83.8108	-7.79	1010
40.1308	-83.7289	-12.52	1095
40.1314	-83.8369	-6.84	1030
40.1317	-83.5778	3.18	1175
40.1328	-83.8547	-8.40	1095
40.1342	-83.8733	-6.52	1157
40.1356	-83.6778	-6.95	1166
40.1392	-83.6456	-1.13	1287
40.1400	-83.6494	-1.85	1262
40.1406	-83.8161	-6.01	1019
40.1414	-83.6308	0.74	1322
40.1419	-83.6361	0.29	1325
40.1419	-83.7089	-11.43	1152
40.1431	-83.7369	-12.54	1084
40.1431	-83.5294	6.98	1060
40.1447	-83.7828	-4.40	1107
40.1456	-83.6800	-6.92	1142
40.1458	-83.6947	-9.03	1145
40.1461	-83.8350	-4.93	1050
40.1469	-83.6017	2.76	1254
40.1494	-83.8531	-4.48	1110
40.1514	-83.5064	8.16	1024
40.1522	-83.6470	-0.20	1283
40.1525	-83.6336	0.52	1324
40.1542	-83.7361	-11.66	1068
40.1542	-83.6822	-6.75	1151
40.1544	-83.7258	-11.46	1084
40.1550	-83.8333	-4.01	1077
40.1550	-83.6972	-9.00	1136
40.1550	-83.6153	1.34	1294
40.1556	-83.7461	-11.39	1062
40.1558	-83.6711	-4.74	1176
40.1558	-83.5283	6.81	1052
40.1558	-83.6022	2.99	1260
40.1564	-83.8147	-4.67	1025
40.1567	-83.8619	-2.33	1130
40.1567	-83.5850	3.92	1198
40.1569	-83.8431	-2.55	1065
40.1572	-83.5911	3.01	1198
40.1578	-83.7847	-9.13	1020
40.1586	-83.7994	-6.31	1026
40.1586	-83.8131	-4.59	1027
40.1606	-83.6850	-7.65	1152
40.1633	-83.5600	5.26	1112

Appendix continued

Latitude	Longitude	CBRA (mgal)	Elevation (feet)
40.1653	-83.6681	-3.61	1175
40.1664	-83.6083	2.45	1190
40.1664	-83.6142	2.81	1183
40.1681	-83.6314	1.68	1184
40.1689	-83.7342	-11.11	1094
40.1692	-83.8608	-0.52	1115
40.1697	-83.7425	-11.20	1080
40.1706	-83.5050	10.31	1022
40.1711	-83.7639	-13.24	1059
40.1711	-83.5978	3.27	1196
40.1722	-83.7822	-8.09	1039
40.1722	-83.7142	-10.27	1111
40.1736	-83.8133	-3.82	1037
40.1739	-83.6472	-1.13	1179
40.1739	-83.5606	6.04	1140
40.1747	-83.8317	-2.48	1056
40.1753	-83.8411	-1.75	1095
40.1761	-83.6139	2.60	1192
40.1767	-83.8592	0.01	1131
40.1775	-83.6267	2.28	1189
40.1792	-83.5850	3.10	1156
40.1800	-83.5461	6.97	1096
40.1803	-83.6911	-7.51	1143
40.1814	-83.6372	1.51	1237
40.1814	-83.5814	2.96	1171
40.1831	-83.6789	-5.71	1169
40.1842	-83.7425	-11.46	1089
40.1844	-83.6708	-4.13	1216
40.1847	-83.7622	-10.93	1146
40.1869	-83.6811	-5.50	1165
40.1878	-83.6958	-8.47	1139
40.1878	-83.7022	-9.59	1117
40.1886	-83.8133	-3.36	1041
40.1889	-83.8203	-2.54	1042
40.1889	-83.7114	-11.11	1167
40.1889	-83.5175	8.88	1045
40.1914	-83.8392	-1.05	1067
40.1914	-83.7419	-11.27	1094
40.1917	-83.7619	-10.43	1155
40.1917	-83.7194	-11.68	1135
40.1917	-83.5572	5.20	1087
40.1925	-83.6511	-0.39	1273
40.1931	-83.6750	-4.96	1174
40.1939	-83.7411	-11.34	1095
40.1944	-83.7806	-7.48	1053
40.1975	-83.6106	2.34	1304
40.1981	-83.8606	1.40	1092
40.1994	-83.8669	2.16	1115

Appendix continued

Latitude	Longitude	CBRA (mgal)	Elevation (feet)
40.1994	-83.6625	-3.94	1274
40.2011	-83.5956	2.85	1239
40.2014	-83.5078	9.69	1025
40.2017	-83.7794	-7.87	1057
40.2022	-83.8664	2.38	1089
40.2025	-83.5342	6.30	1055
40.2031	-83.6672	-4.82	1231
40.2042	-83.7106	-11.54	1169
40.2050	-83.8378	-0.65	1046
40.2058	-83.7392	-11.96	1107
40.2081	-83.6494	-2.43	1204
40.2092	-83.6694	-5.90	1192
40.2094	-83.6342	1.13	1206
40.2094	-83.5389	5.67	1061
40.2106	-83.8183	-2.05	1060
40.2108	-83.7014	-11.13	1186
40.2111	-83.8375	-0.30	1054
40.2111	-83.7092	-11.58	1182
40.2119	-83.6911	-9.57	1169
40.2125	-83.6569	-3.95	1179
40.2125	-83.6147	2.89	1194
40.2128	-83.5747	3.04	1163
40.2136	-83.8656	2.71	1077
40.2150	-83.6819	-8.31	1164
40.2164	-83.7981	-2.19	1091
40.2167	-83.8083	-2.66	1091
40.2175	-83.8169	-1.83	1098
40.2183	-83.8361	0.35	1075
40.2189	-83.7100	-11.01	1197
40.2194	-83.5572	4.03	1096
40.2197	-83.5286	6.25	1040
40.2203	-83.7292	-11.73	1141
40.2203	-83.6592	-5.54	1225
40.2206	-83.6186	0.73	1278
40.2217	-83.7614	-8.81	1072
40.2217	-83.5864	2.99	1184
40.2219	-83.7778	-5.96	1067
40.2233	-83.7064	-10.78	1201
40.2233	-83.5781	3.06	1141
40.2236	-83.6611	-6.73	1289
40.2239	-83.7975	-3.21	1080
40.2264	-83.8444	1.57	1066
40.2281	-83.8642	5.20	1075
40.2281	-83.5236	7.03	1028
40.2289	-83.7078	-10.76	1179
40.2303	-83.5153	8.03	1040
40.2306	-83.7969	-3.04	1107
40.2314	-83.6953	-10.80	1270

Appendix continued

Latitude	Longitude	CBRA (mgal)	Elevation (feet)
40.2317	-83.8156	-0.40	1099
40.2319	-83.5600	3.62	1093
40.2322	-83.6442	-4.49	1358
40.2336	-83.8433	2.14	1098
40.2342	-83.8633	5.48	1088
40.2347	-83.6850	-10.81	1202
40.2356	-83.7281	-10.87	1089
40.2358	-83.7506	-9.16	1085
40.2361	-83.6650	-9.02	1317
40.2361	-83.6439	-5.26	1351
40.2372	-83.6689	-9.15	1297
40.2375	-83.5897	0.57	1180
40.2383	-83.5461	3.38	1060
40.2392	-83.6128	-2.24	1280
40.2397	-83.6500	-6.15	1381
40.2403	-83.7114	-11.38	1187
40.2417	-83.5703	1.48	1136
40.2417	-83.5211	7.60	1032
40.2425	-83.7003	-11.59	1233
40.2433	-83.6953	-10.35	1202
40.2439	-83.6892	-10.61	1306
40.2453	-83.7286	-9.87	1100
40.2458	-83.8139	0.88	1089
40.2461	-83.8039	0.16	1105
40.2461	-83.6281	-3.24	1349
40.2467	-83.7947	-0.83	1126
40.2467	-83.7758	-4.67	1136
40.2469	-83.5239	7.25	1047
40.2481	-83.5353	4.49	1041
40.2483	-83.7847	-2.01	1126
40.2483	-83.7544	-6.96	1086
40.2489	-83.8322	4.11	1082
40.2489	-83.5925	-2.19	1215
40.2494	-83.6650	-9.40	1385
40.2497	-83.5036	9.46	1051
40.2511	-83.7314	-9.32	1100
40.2517	-83.5283	5.00	1040
40.2522	-83.7161	-9.91	1150
40.2522	-83.6544	-8.72	1370
40.2525	-83.7856	-1.35	1119
40.2525	-83.7744	-2.47	1114
40.2550	-83.8669	8.32	1090
40.2550	-83.5808	-1.78	1167
40.2564	-83.7567	-7.05	1110
40.2564	-83.7175	-9.76	1117
40.2567	-83.7300	-9.48	1153
40.2567	-83.6333	-6.03	1293
40.2567	-83.5481	3.14	1050

Appendix continued

Latitude	Longitude	CBRA (mgal)	Elevation (feet)
40.2578	-83.5903	-3.28	1207
40.2581	-83.7089	-10.80	1122
40.2586	-83.8656	8.19	1059
40.2586	-83.5847	-3.37	1166
40.2592	-83.5319	7.58	1072
40.2594	-83.7844	0.07	1108
40.2600	-83.7008	-10.62	1135
40.2606	-83.7922	1.72	1129
40.2608	-83.6611	-9.41	1255
40.2611	-83.8317	4.53	1087
40.2619	-83.8036	1.83	1114
40.2625	-83.8222	3.79	1088
40.2633	-83.8408	5.64	1077
40.2633	-83.5878	-4.19	1191
40.2639	-83.7264	-9.55	1180
40.2647	-83.8586	7.49	1091
40.2656	-83.8653	8.27	1099
40.2656	-83.5564	-1.98	1071
40.2661	-83.6125	-6.18	1289
40.2664	-83.7633	-1.98	1160
40.2664	-83.6781	-9.42	1201
40.2669	-83.7536	-3.45	1103
40.2689	-83.8039	3.31	1127
40.2689	-83.5578	-2.61	1083
40.2692	-83.8211	4.36	1096
40.2692	-83.6056	-6.26	1227
40.2694	-83.7036	-10.47	1150
40.2703	-83.7222	-9.63	1201
40.2719	-83.7731	0.11	1150
40.2719	-83.5419	0.09	1091
40.2722	-83.7669	-0.56	1173
40.2731	-83.7633	-1.09	1171
40.2744	-83.7753	0.37	1135
40.2744	-83.5069	8.57	1097
40.2747	-83.7822	1.42	1128
40.2750	-83.8028	2.94	1132
40.2750	-83.6511	-9.99	1331
40.2758	-83.5642	-4.44	1122
40.2764	-83.8208	4.54	1099
40.2764	-83.6789	-11.58	1220
40.2775	-83.7042	-10.60	1216
40.2777	-83.6014	-6.32	1224
40.2778	-83.8328	5.79	1099
40.2781	-83.8500	7.27	1126
40.2781	-83.8400	6.97	1091
40.2789	-83.8539	7.64	1101
40.2792	-83.8594	7.85	1103
40.2800	-83.8638	7.60	1116

Appendix continued

Latitude	Longitude	CBRA (mgal)	Elevation (feet)
40.2800	-83.7675	-0.64	1142
40.2808	-83.6397	-9.96	1334
40.2817	-83.5964	-6.60	1180
40.2833	-83.6542	-11.34	1367
40.2836	-83.5489	-3.70	1102
40.2850	-83.6086	-9.54	1191
40.2856	-83.6039	-6.93	1200
40.2858	-83.8400	6.30	1090
40.2858	-83.7272	-3.70	1156
40.2864	-83.7056	-7.80	1177
40.2875	-83.5856	-6.94	1155
40.2878	-83.6208	-7.70	1316
40.2883	-83.6881	-10.80	1370
40.2886	-83.7606	-0.70	1192
40.2892	-83.7714	0.20	1150
40.2892	-83.7772	0.30	1143
40.2906	-83.7986	2.09	1117
40.2906	-83.6294	-9.46	1396
40.2911	-83.8078	2.83	1108
40.2914	-83.8131	2.85	1107
40.2914	-83.8217	3.34	1100
40.2919	-83.8294	4.52	1080
40.2942	-83.8525	7.11	1080
40.2942	-83.5883	-7.88	1186
40.2944	-83.8625	7.14	1082
40.2947	-83.5069	2.91	1095
40.2953	-83.6406	-10.52	1470
40.2956	-83.8572	7.35	1080
40.2969	-83.6842	-10.52	1375
40.2981	-83.7314	-2.25	1225
40.2986	-83.5967	-7.61	1248
40.2989	-83.7128	-4.61	1137
40.2994	-83.6614	-10.92	1416
40.2997	-83.6672	-11.58	1388
40.2997	-83.5100	2.18	1074
40.3003	-83.6300	-9.39	1470
40.3008	-83.5639	-6.00	1115
40.3022	-83.5122	1.37	1075
40.3025	-83.7578	-0.86	1210
40.3028	-83.7689	-0.51	1167
40.3031	-83.7800	-0.28	1152
40.3036	-83.5144	0.90	1079
40.3053	-83.7342	-2.24	1226
40.3058	-83.8306	3.85	1059
40.3058	-83.7036	-4.83	1133
40.3067	-83.8322	3.85	1069
40.3078	-83.8556	5.87	1011
40.3083	-83.8086	1.61	1120

Appendix continued

Latitude	Longitude	CBRA (mgal)	Elevation (feet)
40.3083	-83.8500	5.07	1040
40.3092	-83.8747	5.31	1010
40.3097	-83.7019	-5.33	1145
40.3108	-83.6211	-9.66	1429
40.3111	-83.7992	0.21	1112
40.3111	-83.7892	-0.30	1176
40.3128	-83.7369	-6.51	1205
40.3175	-83.7614	-1.64	1194
40.3175	-83.7153	-5.16	1355
40.3178	-83.5197	-1.16	1080
40.3189	-83.7875	-1.60	1190
40.3189	-83.6342	-9.57	1245
40.3197	-83.8072	0.91	1158
40.3208	-83.8306	2.66	1080
40.3211	-83.5828	-7.69	1126
40.3219	-83.6889	-7.78	1159
40.3222	-83.8542	4.08	1077
40.3222	-83.8356	2.76	1071
40.3222	-83.7147	-5.49	1303
40.3233	-83.8447	2.64	1073
40.3239	-83.8739	4.64	1009
40.3239	-83.7300	-4.59	1260
40.3244	-83.5911	-8.72	1164
40.3261	-83.6042	-8.91	1179
40.3278	-83.6625	-10.31	1180
40.3281	-83.7411	-4.10	1254
40.3281	-83.5856	-9.20	1126
40.3281	-83.5294	-3.08	1082
40.3300	-83.5736	-7.02	1101
40.3308	-83.7142	-6.77	1409
40.3322	-83.8342	1.34	1115
40.3328	-83.7761	-2.75	1156
40.3328	-83.5764	-7.22	1101
40.3333	-83.5197	-1.98	1084
40.3344	-83.7953	-0.49	1147
40.3361	-83.7333	-4.42	1350
40.3386	-83.7447	-3.63	1255
40.3414	-83.6239	-10.15	1415
40.3414	-83.5608	-6.21	1088
40.3428	-83.8336	1.03	1106
40.3442	-83.6758	-8.60	1185
40.3444	-83.8419	1.16	1100
40.3444	-83.5458	-5.08	1081
40.3447	-83.8517	1.24	1101
40.3447	-83.7750	-2.29	1185
40.3453	-83.7119	-6.83	1473
40.3458	-83.8722	2.43	1055
40.3481	-83.7425	-3.62	1284

Appendix continued

Latitude	Longitude	CBRA (mgal)	Elevation (feet)
40.3489	-83.7992	-1.14	1143
40.3489	-83.7272	-5.30	1360
40.3489	-83.5161	-2.35	1069
40.3500	-83.8119	0.20	1130
40.3500	-83.6750	-8.33	1223
40.3514	-83.7933	-1.68	1155
40.3517	-83.8411	0.10	1076
40.3525	-83.7078	-6.82	1470
40.3528	-83.8697	1.60	1060
40.3553	-83.5647	-6.65	1090
40.3556	-83.7744	-1.34	1193
40.3558	-83.6564	-9.18	1218
40.3558	-83.6161	-9.58	1322
40.3564	-83.5917	-8.93	1135
40.3569	-83.7761	-2.25	1184
40.3594	-83.8508	0.13	1082
40.3633	-83.7258	-5.54	1473
40.3639	-83.8683	1.02	1052
40.3642	-83.5114	-2.30	1097
40.3650	-83.7064	-6.21	1418
40.3650	-83.6361	-9.40	1253
40.3653	-83.8264	-1.47	1112
40.3656	-83.8406	-0.82	1089
40.3656	-83.8347	-1.12	1101
40.3661	-83.8500	-0.33	1061
40.3661	-83.8108	-2.01	1133
40.3669	-83.8569	-0.13	1058
40.3669	-83.5492	-5.61	1070
40.3675	-83.5278	-4.26	1087
40.3680	-83.7483	-3.49	1330
40.3722	-83.7211	-5.95	1520
40.3725	-83.8708	1.17	1060
40.3733	-83.6142	-9.64	1173
40.3736	-83.6569	-9.21	1460
40.3750	-83.8717	2.16	1052
40.3750	-83.6572	-8.42	1448
40.3758	-83.7050	-5.99	1434
40.3758	-83.6008	-8.54	1125
40.3764	-83.6744	-6.57	1337
40.3778	-83.6781	-5.96	1348
40.3792	-83.6369	-8.72	1327
40.3800	-83.5453	-4.07	1115
40.3817	-83.7708	-3.22	1220
40.3833	-83.6050	-8.48	1132
40.3847	-83.7856	-2.81	1158
40.3850	-83.7892	-2.69	1163
40.3886	-83.7892	-3.23	1149
40.3886	-83.8286	-1.41	1076

Appendix continued

Latitude	Longitude	CBRA (mgal)	Elevation (feet)
40.3889	-83.8481	-0.45	1075
40.3900	-83.7514	-4.95	1322
40.3900	-83.8717	1.43	1046
40.3911	-83.5883	-7.39	1098
40.3917	-83.7167	-4.69	1460
40.3917	-83.6594	-6.54	1434
40.3919	-83.6050	-8.05	1115
40.3928	-83.7931	-3.99	1145
40.3931	-83.6431	-6.94	1332
40.3944	-83.5042	-1.55	1085
40.3947	-83.7703	-3.62	1248
40.3947	-83.5203	-2.98	1070
40.3953	-83.5669	-6.13	1120
40.3956	-83.6972	-4.77	1338
40.3958	-83.8478	-0.34	1094
40.3969	-83.7975	-1.77	1123
40.3975	-83.6767	-5.07	1270
40.4008	-83.6586	-5.55	1388
40.4017	-83.7264	-4.01	1425
40.4022	-83.7475	-4.77	1320
40.4036	-83.7697	-3.76	1230
40.4044	-83.8708	7.93	1041
40.4058	-83.7481	-2.99	1282
40.4064	-83.6592	-6.31	1348
40.4069	-83.6447	-7.28	1313
40.4078	-83.8306	-1.74	1113
40.4092	-83.8461	-0.60	1074
40.4094	-83.5822	-7.37	1116
40.4097	-83.5856	-6.32	1138
40.4103	-83.6164	-8.25	1123
40.4106	-83.6603	-6.48	1303
40.4111	-83.8703	-0.12	1046
40.4133	-83.7008	-4.66	1376
40.4136	-83.7753	-4.03	1199
40.4139	-83.7731	-3.68	1204
40.4150	-83.6639	-5.24	1308
40.4153	-83.8317	-2.16	1074
40.4161	-83.5086	-0.78	1058
40.4183	-83.7542	-4.44	1271
40.4183	-83.7036	-4.41	1386
40.4192	-83.7428	-3.66	1301
40.4219	-83.8092	-3.48	1087
40.4233	-83.8031	-3.94	1117
40.4244	-83.5419	-4.09	1075
40.4247	-83.8514	-1.96	1058
40.4253	-83.8403	-1.87	1052
40.4267	-83.7036	-3.96	1320
40.4275	-83.8272	-2.44	1060

Appendix continued

Latitude	Longitude	CBRA (mgal)	Elevation (feet)
40.4278	-83.6217	-10.17	1150
40.4286	-83.6639	-7.40	1291
40.4300	-83.7967	-3.16	1121
40.4300	-83.5978	-8.71	1110
40.4314	-83.6997	-5.14	1300
40.4333	-83.5642	-5.51	1080
40.4336	-83.7564	-2.47	1251
40.4356	-83.5314	-0.95	1072
40.4358	-83.7369	-2.63	1273
40.4372	-83.8050	-2.60	1083
40.4378	-83.7933	-2.73	1131
40.4386	-83.7814	-3.57	1150
40.4386	-83.7181	-3.75	1303
40.4397	-83.5947	-7.36	1102
40.4400	-83.7667	-12.00	1258
40.4417	-83.8653	-1.71	1037
40.4417	-83.5669	-5.30	1083
40.4419	-83.8542	-1.77	1040
40.4444	-83.8347	-2.50	1042
40.4444	-83.6544	-8.59	1314
40.4456	-83.8306	-3.05	1054
40.4461	-83.6314	-8.38	1170
40.4481	-83.8078	-2.75	1066
40.4494	-83.5903	-6.50	1088
40.4500	-83.8308	-2.64	1047
40.4517	-83.7592	-2.90	1222
40.4522	-83.5678	-3.83	1074
40.4525	-83.8078	-3.10	1062
40.4536	-83.5422	-0.10	1079
40.4553	-83.7900	-2.41	1118
40.4558	-83.7217	-5.74	1198
40.4567	-83.5036	3.99	1064
40.4594	-83.7606	-2.88	1175
40.4619	-83.6578	-7.37	1222
40.4622	-83.6403	-8.27	1171
40.4622	-83.5114	4.63	1062
40.4625	-83.6356	-8.60	1136
40.4633	-83.6286	-8.31	1130
40.4642	-83.7308	-4.89	1161
40.4656	-83.8339	-3.95	1034
40.4656	-83.8114	-4.19	1051
40.4656	-83.7181	-6.92	1175
40.4678	-83.6164	-6.70	1110
40.4681	-83.5792	-3.28	1088
40.4683	-83.5694	-2.66	1078
40.4697	-83.8586	-4.50	1009
40.4706	-83.8403	-4.05	1030
40.4711	-83.5447	1.47	1074

Appendix continued

Latitude	Longitude	CBRA (mgal)	Elevation (feet)
40.4733	-83.5292	4.06	1078
40.4739	-83.7358	-4.55	1141
40.4750	-83.5100	7.60	1058
40.4758	-83.7100	-6.64	1171
40.4772	-83.6850	-6.74	1223
40.4775	-83.7633	-4.81	1069
40.4775	-83.6544	-7.34	1180
40.4781	-83.6742	-7.13	1229
40.4786	-83.7286	-7.02	1140
40.4786	-83.5772	-1.57	1077
40.4794	-83.6522	-6.75	1184
40.4817	-83.8369	-4.68	1016
40.4831	-83.8444	-5.00	1019
40.4833	-83.6314	-7.01	1105
40.4836	-83.8125	-2.72	1037
40.4878	-83.6439	-6.50	1161
40.4878	-83.5772	0.31	1075
40.4892	-83.5461	3.41	1059
40.4906	-83.7653	-5.69	1040
40.4906	-83.5322	4.88	1057
40.4914	-83.7411	-7.09	1063
40.4919	-83.8386	-4.99	1015
40.4925	-83.5189	7.29	1060
40.4928	-83.6211	-5.63	1106
40.4947	-83.6994	-8.55	1151
40.4956	-83.5969	-1.51	1087
40.4969	-83.5731	1.11	1074
40.4986	-83.6578	-7.02	1151
40.4992	-83.7428	-8.43	1053
40.4997	-83.8397	-13.81	1004